EUROPEAN COMMISSION

Community research

Monitoring Developments for Safe Repository Operation and Staged Closure

Contract Number:232598

Wireless Data Transmission Demonstrator: from the HADES to the surface (D-N°:3.4.2)

Author(s): **T.J. Schröder, E. Rosca-Bocancea, NRG**

Date of issue of this report : **31/10/2013**

Start date of project : **01/05/2009** Duration : 54 Months

Project co-funded by the European Commission under the Seventh Euratom Framework Programme for Nuclear Research &Training Activities (2007-2011)		
Dissemination Level		
PU	Public	x
RE	Restricted to a group specified by the partners of the MoDeRn project	
CO	Confidential, only for partners of the MoDeRn project	

EURATOM

History Chart			
Type of revision	**Document name**	**Partner**	**Date**
First draft	MoDeRn D342 NRG-Hades v0.doc	NRG	6/9/12
Final internal draft	MoDeRn D342 NRG-Hades draft1.docx	NRG	14/5/13
Review	MoDeRn D342 NRG-Hades draft1 _bbreview	NDA	16/7/13
Final draft	MoDeRn D342 NRG-Hades final draft.docx	NRG	3/10/13
Final draft review	MoDeRn D342 NRG-Hades final draft bb_minor edits.docx	NDA	7/10/13
Final version	MoDeRn D342 NRG-Hades final.docx NRG report NRG-22336.34/13.122669	NRG	8/10/13

Table of Contents

Executive Summary

The retrievability of waste from a geological disposal is a basic principle of the Dutch radioactive waste management policy [1, 2]. An important aspect in this is to realize tools on the basis of which decisions can be made for a possible retrieval of already emplaced waste containers from a (partially) closed repository. One such tool is the in-situ monitoring of parameters that indicate the evolution of the disposal system. When the in-situ monitoring in a geological radioactive waste disposal facility is continued into the post-closure phase (i.e. when the access shaft is closed), an autonomous subsurface monitoring infrastructure is needed. To be able to evaluate the monitoring data collected in the deep geological disposal facility, the data must be transmitted to the surface by a wireless transmission technique.

As part of the FP7-project *MoDeRn* [3], NRG worked on the wireless transmission of data by low-frequency magnetic fields. The transmission of data over larger distances (>100 m) through an electrically conductive medium is challenging, because transmission by magneto-inductive techniques can only be realized at unfavourable low frequencies usually avoided for communication. The HADES Underground Research Laboratory (URL) situated in Mol, Belgium, was found to be a very suitable location for demonstrating the feasibility of this technique under conditions expected for the Dutch generic disposal concept in Boom Clay: the high electrical conductivities of the transmission path between the HADES and the surface are comparable to the Dutch Case. The long-term, stand-alone energy supply inside the repository is identified as a potential limiting factor in a post-closure situation, therefore the main objective of NRG's contribution is to characterize and optimize the energy use of the wireless technique within the specific context of post-closure monitoring. This should help to judge the principal feasibility of long-term wireless data transmission from an underground repository through the surrounding host rock and the overlying geosphere to the surface.

In this report, the experimental work, performed by NRG at the HADES URL as part of the *MoDeRn* Work Package 3.4, is presented. The main objective of this work is the demonstration of the feasibility of wireless data transmission from a geological disposal to the surface under conditions representative for the Dutch generic concept in Boom Clay [7]. The concepts developed by NRG in the *MoDeRn* Deliverable D.2.3.1 [8] have been used to define the overall set-up and to make technical selections for individual components. Efforts have been made to optimize the set-up within the specific limitations of the HADES, and additional measurements were executed at other locations in order to demonstrate that under more ideal conditions better performances can be achieved, in line with analyses performed in [8]. Some uncertainties discussed in [8] are evaluated experimentally during the field experiments at the HADES, including the electrical conductivity of the subsurface and the propagation behaviour beyond (static) near-field conditions. Gained experimental results are compared with the theoretical foundation developed in [8].

The experimental results demonstrated that by careful system design, data transmission through 225 m of a highly conducting geological medium is feasible: NRG has demonstrated at the HADES the wireless transmission of data through 225 m of an electrically highly conductive geological medium

(Boom Clay and overlying sandy aquifers), at frequencies up to 1.7 kHz and with data rates up to 100 sym/s.

The outcomes of the data transmission experiments were found to be consistent with the theoretical framework developed in WP2.3 [8]. The analyses performed in [8] showed that, although some uncertainties exist and some parameters need to be obtained experimentally, the framework developed permits estimation of general features and parameters required for the set-up of a transmission chain from a subsurface disposal facility to the surface. One of the major uncertainties identified was the propagation behaviour of the subsurface antenna in the extended near-field of a conducting half space[1]. Experiments performed at the HADES showed that although the field vector differed from what was implied by the approximation equation used, the overall field strength is in close agreement with what was expected (within less than a factor of two).

The amount of energy required to transmit data to the surface was within expectation, although due to the local conditions in Mol, (limited space in the underground facility, strong interference above ground) the capability to demonstrate the expected efficiency of the technique was limited. The overall efficiency of the developed technique was found to be quite promising: with 1 Ws/bit demonstrated under the very challenging conditions present at the HADES, a few mWs/bit extrapolated from additional surface-surface experiments performed in a recreational area, and less than 1mWs/bit expected under more optimal conditions. Based on the calculated energy use and the expected amount of data to be transmitted, it can be concluded that in principle, the technique used can transmit data from underground to surface during the post-closure phase of a deep geological disposal facility. Estimation of the energy need in the case of the Dutch generic disposal concept in Boom Clay, situated at 500 m depth, results in less than 1 mWs of energy per bit of transmitted data. In other host rocks (rock salt, granite, Opalinus clay), even higher energy efficiencies could be achieved due to lower electrical conductivities of the subsurface. However, one still may feel some need to provide additional experimental evidence for the enhanced efficiency of the technique when a larger antenna is applied. This aspect has been evaluated in this report, but it would require a different location than the HADES, preferentially at a relevant depth (>250 m) and with sufficient space to place a transmitter antenna of relevant dimension (loop radius >0.1 transmission distance).

While the current studies provides evidence for the feasibility of data transmission over longer distance after closure, additional work need to be performed in order to allow a solid statement on the technical feasibility of post-closure monitoring. This includes the long-term supply, i.e. over several decades, of power to the data transmission system and other components of the autonomous subsurface monitoring system, the reliability and performance of the monitoring components after closure, and the integration of different technologies used [4].

[1] a *'conducting half space'* describes in geophysics a situation where the receiving antenna is situated at the boundary between a conducting medium (subsurface) and a non-conducting medium (air)

List of Acronyms

BER:	Bit error rate
BPSK:	Binary phase shift keying
CFD:	Cumulative frequency distribution
DFT:	Discrete Fourier Transformation
EM:	Electro-magnetic
GSM:	Global System for Mobile Communication
HADES:	High-Activity Disposal Experimental Site
HLW:	High-level waste
IAEA :	International Atomic Energy Agency
ILW:	Intermediate-level waste
LLW:	Low-level waste
PSK:	Phase shift keying
RTD:	Research and Technological Development
TECDOC:	Technical Document
URL:	Underground Research Laboratory
WP:	Work package

List of Key Terms

Post-closure monitoring, through-the-earth data transmission, low-frequency magneto-induction, magnetic field propagation, demonstrator, HADES URL, underground research laboratory

1 Introduction

The successful implementation of a repository programme relies on both the technical aspects of a sound safety strategy and scientific and engineering excellence, as well as on social aspects such as public acceptance. Monitoring has the potential to contribute to both of these aspects and thus may play an important role as national radioactive waste disposal programmes move forward towards a successful conclusion, i.e. safe and accepted implementation of geological disposal.

The role of monitoring through the staged implementation of geological disposal has been considered on an international basis through production of an International Atomic Energy Agency (IAEA) Technical Document (TECDOC) on monitoring of geological repositories [5] and by the European Commission (EC) within a Thematic Network on the Role of Monitoring in a Phased Approach to Geological Disposal of Radioactive Waste [6]. These two documents have given a first description how monitoring can support the implementation of geological disposal in a broad sense. Following the line of these documents, the main objective of the EC Seventh Framework Programme "Monitoring Developments for Safe Repository Operation and Staged Closure" (*MoDeRn*) Project is to further develop the understanding of the role of monitoring in staged implementation of geological disposal to a level of description that is closer to the actual implementation of monitoring.

Work in the *MoDeRn* Project is undertaken in a comprehensive and coherent programme of research structured into six interrelated work packages:

- **Work Package 1: Monitoring Objectives and Strategies:** Work Package 1 will provide a clear description of monitoring objectives and strategies that (i) appear suitable in a given physical and societal context, (ii) may be implemented during several or all phases of the radioactive waste disposal process, (iii) appear realistic in light of available monitoring technology, (iv) take into account feedback from both expert and lay stakeholder interaction, and (v) provide information to support decision-making processes, while developing the licensing basis.

- **Work Package 2: State-of-the-art and RTD of Relevant Monitoring Technologies:** The second work package will result in a description of the technical requirements on monitoring activities as well as an assessment of the state-of-the-art of relevant technology responding to these requirements (the subject of this document); it includes a technical workshop involving other monitoring Research and Technological Development (RTD) projects, leading to the identification of RTD techniques that enhance the ability to monitor a repository.

- **Work Package 3: *In situ* Demonstration of Innovative Monitoring Technologies:** The third work package will develop *in situ* demonstration of innovative monitoring techniques and provide a description of innovative monitoring approaches specifically responding to some of the design requirements of a repository.

- **Work Package 4: Case Study of Monitoring at All Stages of the Disposal System:** The fourth work package will be dedicated to a series of case studies illustrating the process of mapping objectives and strategies onto the processes and parameters that need to be monitored in a given context, the possible design of corresponding monitoring systems, possible approaches to prevent and detect measurement errors, and the handling of "unexpected" repository evolutions.

- **Work Package 5: Dissemination of Results:** The fifth work package will provide a platform for communicating the results of the *MoDeRn* Project. Two international meetings will be held, an international workshop with safety, regulatory and advisory authorities to communicate current state-of-the-art monitoring approaches and to engage expert stakeholders in the further development of repository monitoring objectives and strategies, and an international conference on repository monitoring. The work package also includes production and maintenance of a project web site.

- **Work Package 6: Reference Framework:** The final work package will consolidate results from the previous work packages and provide a shared international view on how monitoring may be conducted at the various phases of the disposal process. Early work in the *MoDeRn* Project has contributed to the reference framework by drafting a generic structured approach to monitoring - the *MoDeRn* Monitoring Workflow, which provides a methodology for developing and implementing a monitoring programme under specific national boundary conditions.

1.1 Scope of this report

The retrievability of waste from a geological disposal is a basic principle of the Dutch radioactive waste management policy [1, 2]. The implementation of this policy can be achieved by an appropriate repository concept and by procedures in the waste management strategy. The present Dutch repository concept comprises a generic disposal facility for both HLW and ILW/LLW at a depth of 500 m in Boom Clay, which is abundantly present in the subsurface of the Netherlands [7]. An important aspect in this is to realize tools on the basis of which decisions can be made for a possible retrieval of already emplaced waste containers from a (partially) closed repository. One such tool is the in-situ monitoring of quantities that indicate the evolution of the disposal system.

When the in-situ monitoring of a geological radioactive waste disposal facility is continued in the post-closure phase (i.e. when the access shafts are closed), an autonomous subsurface monitoring infrastructure is needed. To be able to evaluate the monitoring data collected in a deep geological disposal facility, the data must be transmitted to the earth's surface by a wireless transmission technique. For the wireless transmission of data, high-frequency electromagnetic waves are used in many applications. Electromagnetic waves can be transmitted easily over larger distances in air, but the presence of solid objects is known to potentially impede the wave propagation. The application of high frequency techniques in a geologic waste disposal is therefore limited to short distances (few meters to tens of meters). When it comes to the wireless transmission of data between different sections of a deep geological repository or between a repository and the surface, the large attenuation of the signal by several hundred meters of geologic medium makes the application of high frequency waves impractical.

As part of the FP7-project *MoDeRn* [3], NRG worked on the wireless transmission of signals and data by low-frequency magnetic fields, that are judged to be more suitable for the transmission over long distances through an electrically conducting, solid material. Because the long-term, stand-alone energy supply inside the repository is identified as a potential limiting factor in a post-closure situation, the main objective of NRG's contribution is to characterize and optimize the energy use of the wireless technique within the specific context of post-closure monitoring. This should help to judge the principal feasibility of long-term wireless data transmission from an underground repository through the surrounding host rock and the overlying geosphere to the surface.

Because only a limited amount of information exists about the application of low-frequency magnetic field for the purpose of data transmission, NRG performed RTD activities as part of the *MoDeRn* Work Package 2.3. The outcomes are reported in the *MoDeRn* Deliverable D.2.3.1 [8] and summarize the main principles behind this technology, focussing on all aspects that are relevant for the intended application. Basic physical and technical principles were analysed with respect to an energy efficient design, and the results were used to design and build the equipment required to transmit data from the Belgian underground research facility (HADES URL) to the surface.

In this report, the experimental and demonstration work performed by NRG at the HADES as part of the *MoDeRn* Work Package 3.4 is presented. The main objective of the NRG contribution is the demonstration of the feasibility of wireless data transmission from a geological disposal to the surface under conditions representative for the Dutch generic concept in Boom Clay [7]. The concepts developed in the *MoDeRn* Deliverable D.2.3.1 [8] are used to define the overall experimental set-up and to make technical selections of individual components. Efforts are made to optimize the set-up within the specific conditions present in the HADES, in line with the analyses performed in the *MoDeRn* Deliverable D.2.3.1, and additional measurements were performed on other locations to demonstrate the high performance of the method achievable under more ideal conditions, Some uncertainties identified in [8] were evaluated experimentally during the field experiments at the HADES: the electrical conductivity of the subsurface and the propagation behaviour beyond near-field conditions. Experimental results gained are compared with the theoretical foundation developed in the *MoDeRn* Deliverable D.2.3.1.

In the next chapter, the experimental set-up used at the HADES is described, discussing each of the individual components of the transmission chain. In Chapter 3, the results of the transmission experiments are summarized. Chapter 4 provides an analysis of the energy need based on the work in this report and the analysis presented in the *MoDeRn* Deliverable D.2.3.1 [8] and extrapolates the results - where necessary - to the application case. In Chapter 5, final conclusions are provided. The main principles of magnetic field propagation, as worked out in the D.2.3.1 report, can be found as a condensed summary in Appendix A.

2 Experimental set-up

In this chapter, the components of the transmission chain are summarized and discussed with respect to their relevant features. The principal components of the transmission chain are summarized in Figure 1 below. The relevant features of the components are analysed and most components are tailor-made by NRG for the specific applications. Before elucidating the individual components of the transmission chain (Sections 2.2 to 2.7) a description of the research location at Mol and its relevant subsurface characteristics is provided. Details of the performed experiments are described in Sections 2.8 and 2.9.

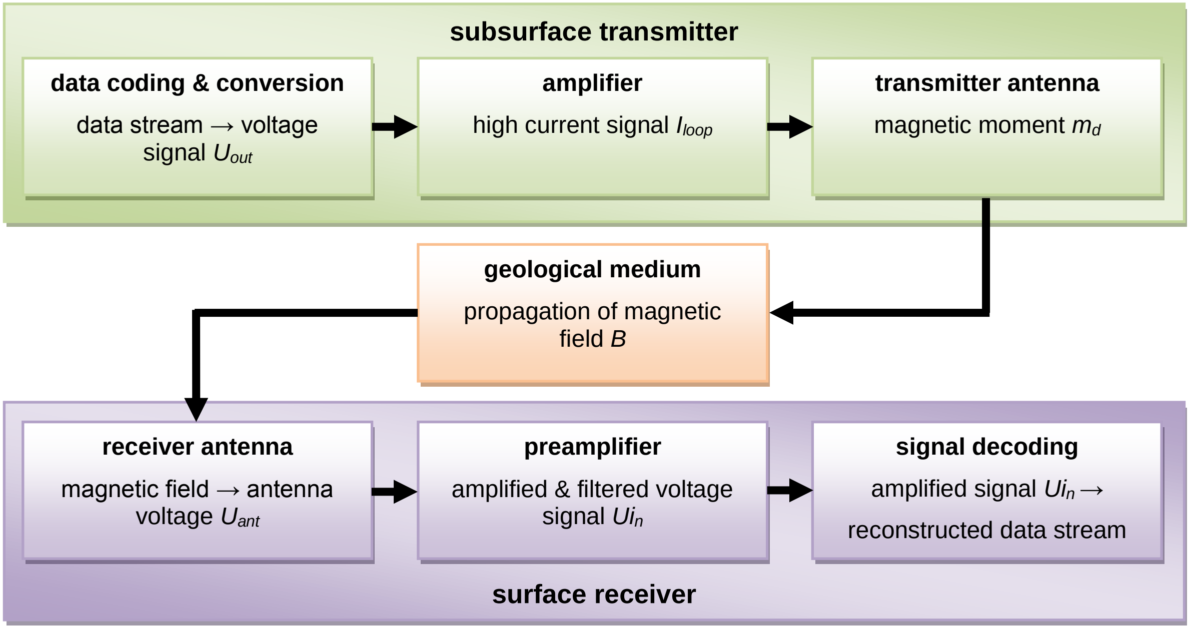

Figure 1: Overview of the principal components of the transmission chain.

2.1 Description of the research location & transmission path

The demonstration works performed by NRG are mainly done at the High-Activity Disposal Experimental Site Underground Research Laboratory (HADES URL) in Mol, Belgium, managed by *ESV EURIDICE*. The HADES consists of a single gallery of more than 80 m length, situated at a depth of 225 m below surface, in a layer of Boom Clay. The newer part of the HADES gallery was used for the NRG transmission experiments and has an inner diameter of 4 m.

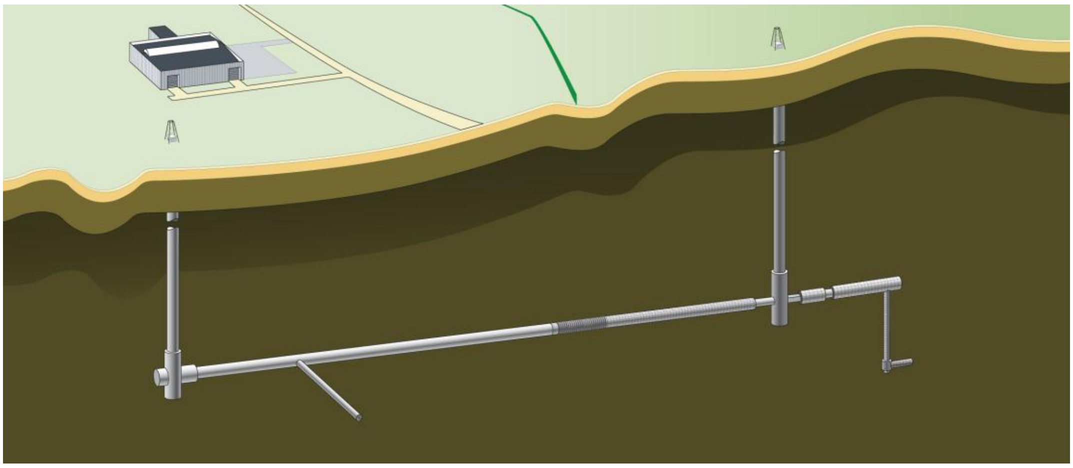

Figure 2: Underground Research Laboratory HADES in Mol, Belgium. ©EIG EURIDICE.

Figure 3 shows the location of the surface receiver and subsurface transmitter. The receiver antenna is located about 10 m off-axis of the HADES, in a green field next to the connecting road.

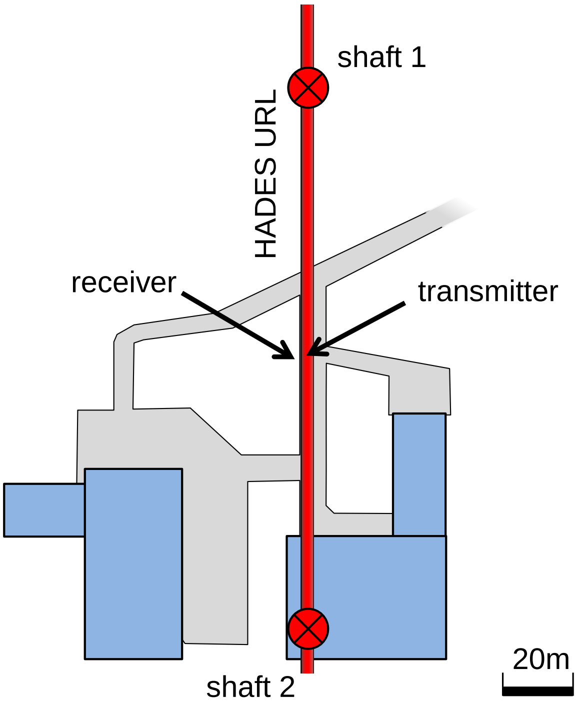

Figure 3: Location of the subsurface transmitter and surface receiver at the *EURIDICE* site in Mol, Belgium (red: HADES, blue: *EURIDICE* buildings, grey: roads & parking spaces).

As discussed in [8], the electrical conductivity of the subsurface is a relevant parameter for quantifying the propagation of magnetic fields: in electrically good conducting media, magnetic fields are increasingly attenuated with increasing penetration depth by the generation of eddy currents and secondary fields [9]. The conductivity has a relevant impact on the achievable transmission frequency, and thus the overall energy efficiency of the technology. In [10], an electrically conductivity of about 0.2 S/m for the first 10 m of Boom Clay above the HADES is reported, decreasing to a value of about

0.1 S/m within the next 25 m of clay (Figure 4). The conductivity of the overlying 190 m of sandy layers ranges from about 0.02 to 0.05 S/m [11]. The effect of stratification on the overall propagation behaviour was estimated in [12]. On basis of the example calculations there, a conductivity value for the overall transmission path (Eq. 10 to Eq. 12 in Appendix A) was approximate by graphical integration of the resistivity values in [11], leading to a best estimate of the overall conductivity of 33 mS/m.

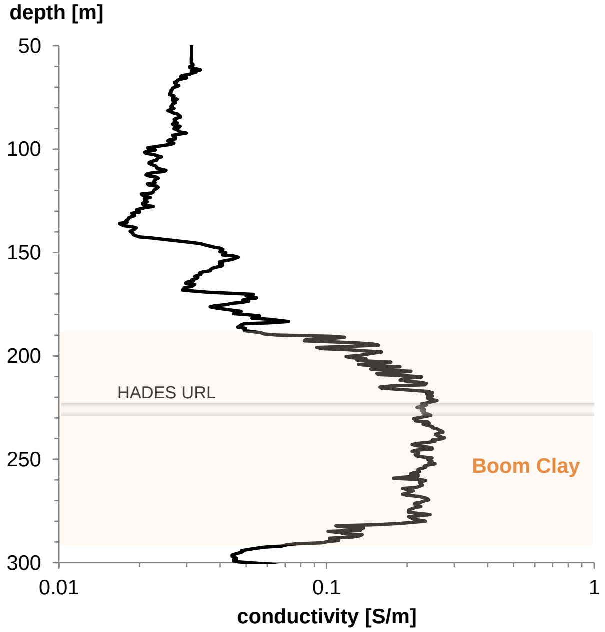

Figure 4: Conductivity of the subsurface at Mol (adapted from [11]).

Although the depth of HADES facility is only half of the depth of the Dutch generic disposal concept [7], the high electrical conductivity values of the host rock and the overburden are very representative for the Dutch situation[2]. One of the main uncertainties identified, the propagation behaviour in the extended near-field [8], is directly related to the conductivity and strongly affects the maximum achievable transmission frequency. The high conductivity makes the HADES a very suitable experimental location in order to investigate propagation behaviour beyond near field conditions and to demonstrate data transmission under these very challenging conditions. With respect to the extrapolation of experimental results to the greater depth of the Dutch disposal concept, this can be performed on basis of the information provided in [8], supported by an evaluation of measured propagation behaviour at the HADES (Section 3.1.2).

In Figure 5, transfer functions for magnetic field propagation for the relevant conductivity range between 0.1 and 0.02 S/m as expected at the HADES are depicted (see also [8]), showing that optimum transmission frequencies for the experiments can be expected between 400 Hz and 2.5 kHz[3].

[2] note that the electrical conductivity of other host rocks, i.e. rock salt, granite or non-plastic argillaceous rock as Opalinus clay are much lower

[3] note that the transfer function for data transmission as discussed in [8] does not apply here, because the used loop antenna will be much smaller than the optimum loop size

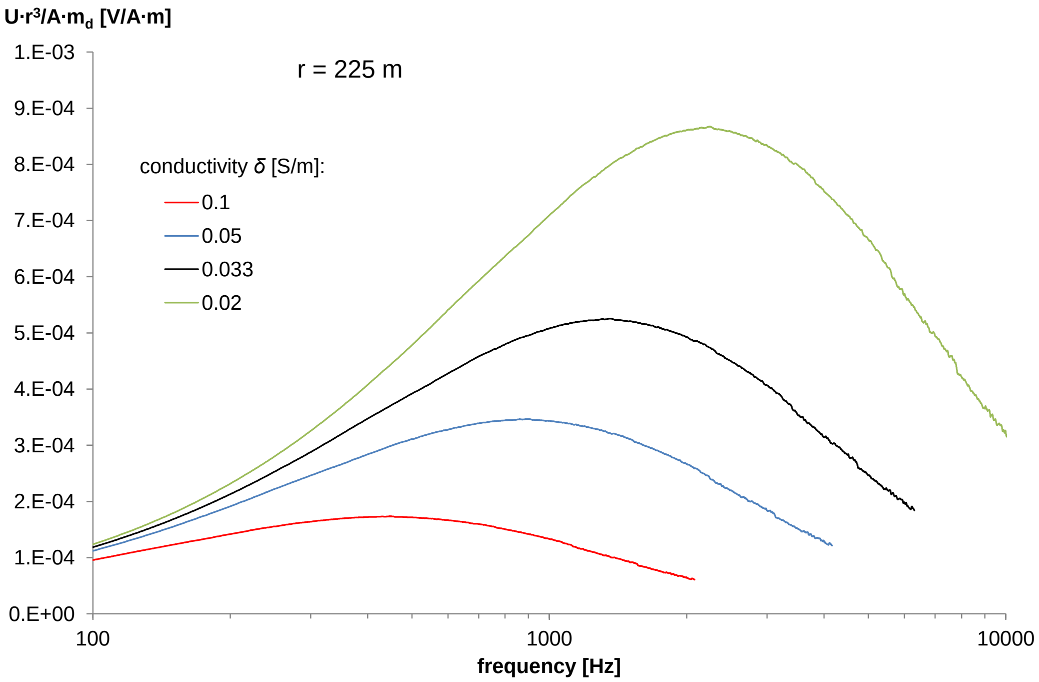

Figure 5: Transfer function for magnetic field propagation through a conducting medium for a resonating transmitter antenna, a transmission distance of 225 m and electrical conductivities between 0.1 and 0.02 S/m.

When investigating other location-specific boundary conditions, the experimental conditions at Mol are found to be suboptimal with respect to three features:

- The size of the transmitter antenna is limited by the diameter of the HADES, leading to an antenna aperture far below optimum. Based on the transmission distance, the optimum antenna aperture is >100'000 m^2, with an antenna inductivity that allows the transmission of about 50 sym/s at 1.5 kHz/2Ω. Comparable data transmission performances with transmitter loops of 4 m diameter or less result in an antenna aperture of less than 200 m^2.
- Due to the presence of several on- and off-site power-lines, strong interferences exist on the surface above the HADES URL. These interferences affect the experiments in four ways:
  - The background noise levels are substantial;
  - The large signal strength lead to demanding requirements for the equipment used with respect to linearity, dynamic range and frequency separation;
  - Data transmission bandwidth is limited;
  - Variability of interference patterns cannot always be anticipated, leading to some risk that an experimental set-up based on previous measurements may lead to suboptimal performance a next measurement campaign
- Experimental work is performed during daytime, leading to additional transient interferences (e.g. by passing cars, operation of the shaft lift). These factors/interferences affect the ability to perform statistical analysis of the experimental results as, for the proper quantification of the performance of coding methods, very long (undisturbed) time intervals are needed. E.g. for a symbol rate of 20 sym/s, about one and a half hour are required to transmit 100'000 symbols, which is considered the minimum amount of data to permit the evaluation of bit-error rates of 0.1% in a proper way.

2.2 Data coding & conversion

The pulsed sinusoidal signals and data streams used for the experiments are generated by software, and loaded as uncompressed *.wav* files to a MP3-player that serves as signal source. As discussed in [8], the influence of the data coding & conversion unit is judged to be irrelevant to the overall energy efficiency of the technique. The choice of methods and equipment was therefore based on practical aspects related to the experiments at the HADES only, and no measurements of energy use were performed.

For the characterization of the propagation behaviour of the geological medium, pulsed sinusoidal signals in the frequency range between 200 Hz and 5 kHz (Figure 5) were used, with a pulse length between two and five seconds. For the data-transmission experiments, differential binary phase shift keying (BPSK) was used in order to modulate *Varicode*-coded text-strings (see Section 3.2.1). The transmission channels used ranges between 1.0 and 1.7 kHz, and were based on the evaluation of local background noise pattern (see Section 3.1.1 and 3.1.3). Symbols rates ranged from 3 sym/s to 100 sym/s.

2.3 Transmitter amplifier

For the HADES experiments, commercial available so-called *Class-D* amplifiers were used. Due to the high energy needs expected as result of the (unfavourable) local circumstances present at the HADES, the selected frequency range and the need for high linearity, two amplifier were purchased that could provide sufficient power (>200 W) into a minimum load of 2 Ω, one fed by a rechargeable battery and the other fed by the 220 power network. For the additional experiments performed in a recreational area close to the NRG site in Petten (see Section 2.9), no amplifier was necessary: for these experiments, the signal source (MP3-player) was directly connected to the transmitter antenna, providing about 1 mW to the antenna[4].

As discussed in [8], the energy efficiency of Class-D amplifiers depends on the selected output power, but because the output power required at the HADES is not at all representative for a disposal situation the power efficiency of the selected amplifiers were not measured.

2.4 Transmitter antenna

As discussed in Section 2.1, the dimensions of the transmitter antenna were limited by the diameter of the HADES gallery, resulting in the application of circular or octagonal antennas with 3.4 m to 3.65 m diameter. In order to increase the antenna aperture, multi-turn loops of copper wire were used. Because the inductivity increases with the square of the number of turns (Eq. 9 in Appendix A), the high inductance of the multi-loop antenna results in relevant contributions to the overall impedance in the projected frequency range (Eq. 8 in Appendix A). In order to perform both signal transmission experiments at larger frequency intervals (200 Hz - 5 kHz) and data transmission experiments at single frequencies under optimum conditions, several transmitter antennae were designed and built by ECN and NRG. An overview of the transmitter antenna parameters are given in Table 1. Note that

[4] in order to adapt the load resistance to the MP3-players specification, a serial resistor of 21.5 Ω was used

transmitter antenna NRG-1 is used for calibration purposes only. Figure 6 and Figure 7 show the transmitter antennas ECN-1 and NRG-3 in the HADES, respectively.

Table 1: Overview of transmitting antenna parameters

parameter	ECN-1	NRG-1	NRG-2	NRG-3
antenna topology	octagonal loop	solenoid	circular loop	circular loop
loop radius r_l	1.75 m	0.042 m	1.7 m	1.8 m
number of turns N	39	79	6	9
antenna aperture	380 m^2	0.43 m^2	54.5 m^2	94.0 m^2
wire diameter d_w	1.8 mm	0.8 mm	0.6 mm	1.06 mm
electrical resistance R_{res}	3.0 Ω	0.72 Ω	4.1 Ω	2.1 Ω
antenna inductivity L	17.5 mH [b]	*n.d.*	0.5 mH [a]	1.2 mH [b]
mass of copper m	8 kg	<0.2 kg	0.2 kg	0.8 kg

[a] estimated from geometry; [b] measured at HADES

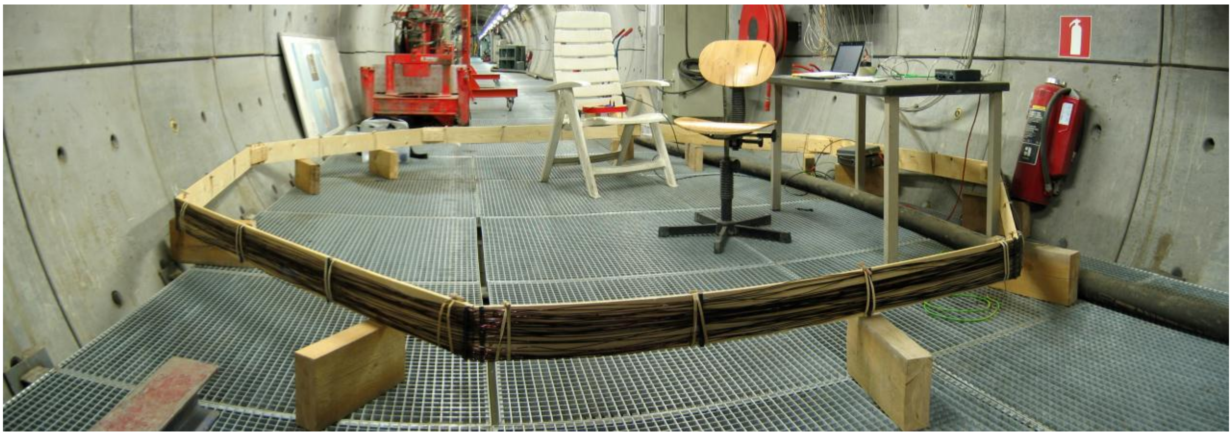

Figure 6: Transmitter antenna ECN-1 in the HADES URL.

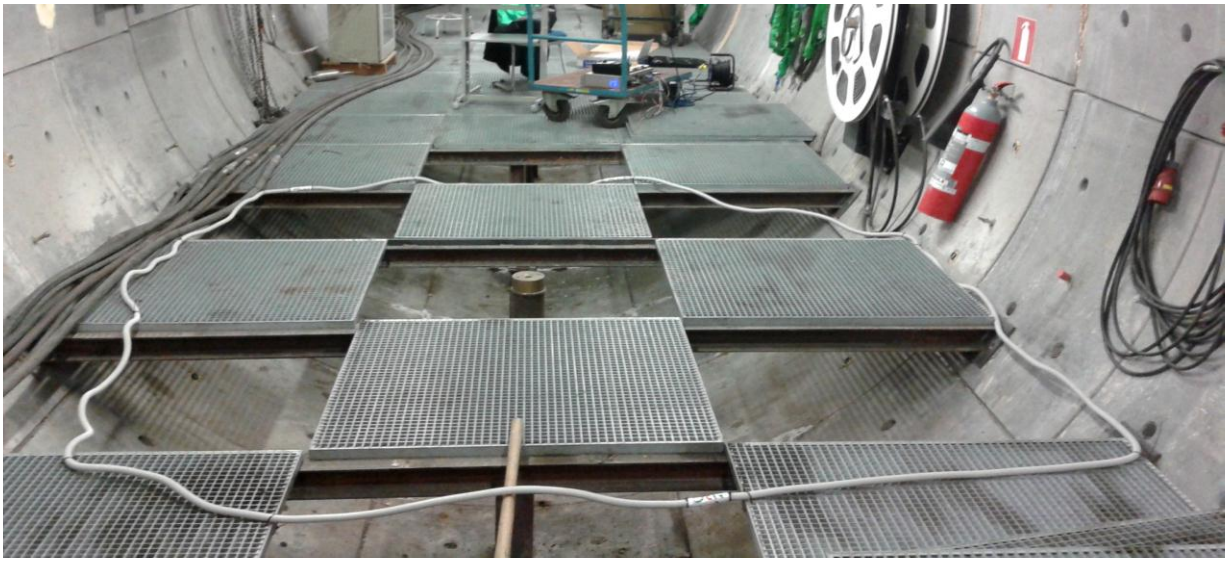

Figure 7: Transmitter antenna NRG-3 in the HADES URL.

2.5 Receiver antenna

Several potential sensor techniques exists to detect magnetic fields. SQUIDS, fluxgate magnetometers, and loop antennas (or 'search coils') are identified as the most sensible technologies. Of these techniques, the loop antenna was selected as the most appropriate technology for the intended experiments (see [8]). Several loop antenna designs were built and their principal features were tested.

The main criteria for the receiver antenna design are a large sensitivity, low noise, high linearity, and a sufficient low capacity that does not interfere with the intended frequency range. Additionally, for this study, the overall dimensions of the antenna are of interest for two reasons:

- Large antenna dimensions are more vulnerable to interferences in the radio frequency (RF) range with cm to dm wave length: when the inductivity of a single turn interacts with the capacity between two turns, this can result in an efficient resonance circuit in the frequency range between 10 MHz and 1 GHz.
- A set of two receiver antennas had to be repeatedly transported from the Netherlands to Mol by car.

Table 2 summarizes the properties of several receiver antennae tested. In general, a single-layer solenoid was considered as an optimum design with respect to linearity and low capacity. The antenna NRG-4 was designed as a compromise between high sensitivity and practical considerations discussed above and was built in twofold in order to measure simultaneously vertical and radial field components. However, the large physical dimensions of the antenna NRG-4 make use inside the HADES URL less feasible: because of the presence of magnetically-permeable material in the HADES (e.g. floor grid, rails for cables), magnetic field vectors are expected to be locally very variable. For potential experiments in an upside-down configuration, where the receiver antenna will be situated inside the HADES URL, additionally a ferrite loop antenna (NRG-3) was constructed. Besides, the antenna was used to test the relevance of magnetic hysteresis on noise properties and data transmission performance.

Table 2: Overview of receiving antenna parameters

parameter	ECN	NRG-1	NRG-2	NRG-3	NRG-4
antenna topology	flat disk	solenoid	ferrite loop	ferrite loop	solenoid
solenoid diameter d_l	0.21 - 0.27 m	0.13 m	0.01 m	0.01 m	0.4 m
solenoid height h_l	2 cm	0.14 m	0.12 m	0.12 m	65 cm
number of turns N	1000	1060	~725	~2500	900
antenna aperture	44 m^2	13.8 m^2	~6 m^2	~20 m^2	117 m^2
electrical resistance R_{res}	33.5 Ω	594 Ω	6.2 Ω	46.5 Ω	71 Ω
antenna inductivity L	260 mH	120 mH	~45 mH	500 mH	175 mH
sensitivity at 1 kHz	0.28 µV/pT	0.09 µV/pT	0.04 µV/pT	0.13 µV/pT	0.63 µV/pT
mass of copper m	2.8 kg	<0.2 kg	<0.2 kg	<0.2 kg	2.9 kg

Figure 8 show the receiver antenna NRG-4.

Figure 8: Receiver antenna NRG-4 at the surface in Mol, above of the HADES URL.

2.6 Receiver amplifier

For the amplification of the receiver antenna signal, NRG designed and built several dedicated preamplifiers. The main objective was to construct preamplifier with a defined bandwidth and the highest achievable sensitivity (see [8]). Other design criteria were: a high dynamic range that enables strong local interferences to be addressed; adaption to the low resistance, high inductive input load of the receiver antenna (see Table 2); the possibility of early removal of unwanted frequencies in the circuit in order to avoid oversteering by strong local interferences present in Mol (see Section 3.1.1); and a linear group delay. Figure 9 to Figure 11 show the transfer functions and noise spectrums of the designed preamplifiers, and Table 3 and Figure 13 summarize the achieved sensitivity of the preamplifiers respectively based on the input noise and loop antenna measurements with receiver antenna NRG-4.

A prototype preamplifier with a high fixed gain (NRG-1, Figure 9) was used in the first experiments, but appears to be not optimal due to the strong local interferences that oversteered the ADC under certain conditions. Two additional preamplifiers, one with a larger bandwidth (NRG-2, Figure 10) and one with a smaller bandwidth (NRG-3, Figure 11) were built allowing the simultaneous measurement of vertical and radial field components. These preamplifiers have a smaller gain than NRG-1v4 (see Figure 9 to Figure 11), and additionally the variable gain of the ADC preamplifier was used in order to optimize signal-noise for the individual measurements/antenna set-ups. To reduce interferences as much as possible during experimental work, the bandwidth of the preamplifiers was eventually adapted in several steps for the different measurement campaigns, starting with the identified range of 200 Hz to 5 kHz, and narrowed to the relevant range for each experiment (indicated as NRG-1v1, NRG-1v2, NRG-1v3, etc.)

Table 3: Sensitivity of the receiver preamplifiers NRG-1v4, NRG-2v3, and NRG-3v3, and the ADC in the frequency range of 1 - 2 kHz

preamplifier	input noise
ADC	68 nV/√Hz
NRG-1v4	4.0 nV/√Hz
NRG-2v3	1.4 nV/√Hz
NRG-3v3	1.4 nV/√Hz

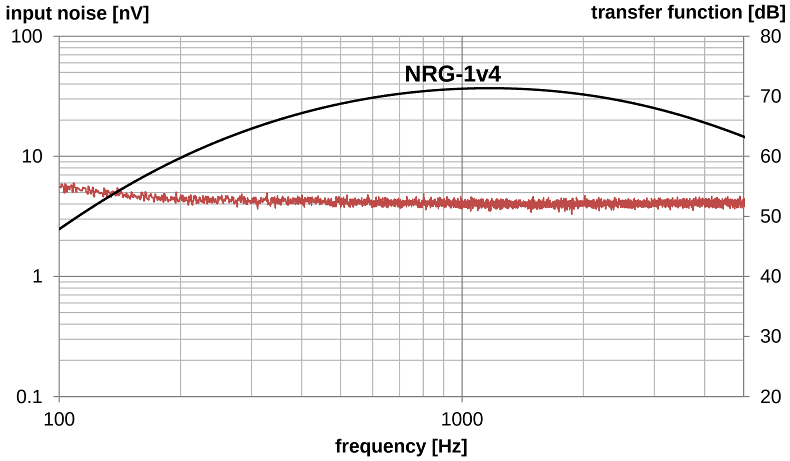

Figure 9: Transfer function (black line) and measured input noise (red line) of the receiver preamplifier NRG-1v4.

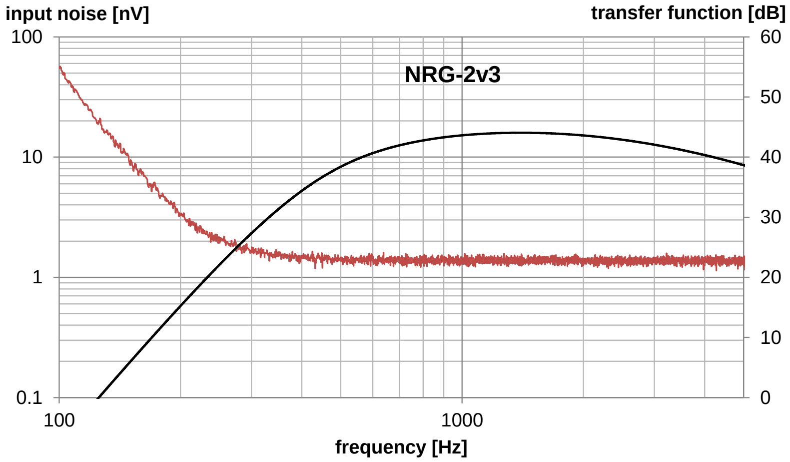

Figure 10: Transfer function (black line) and measured input noise (red line) of the receiver preamplifier NRG-2v3.

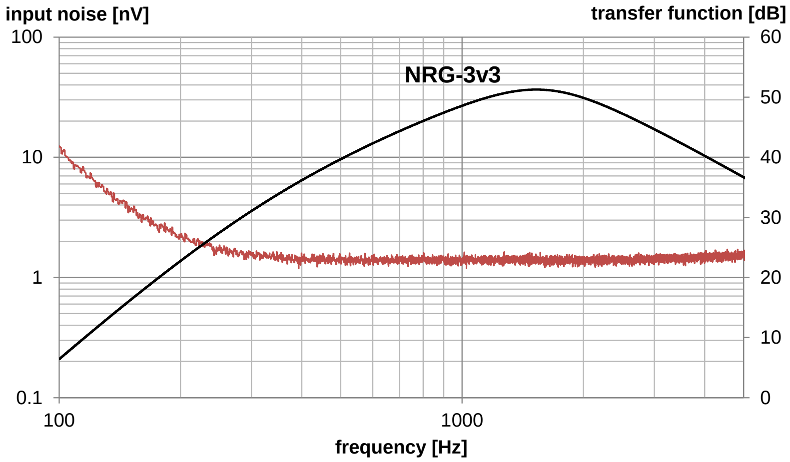

Figure 11: Transfer function (black line) and measured input noise (red line) of the receiver preamplifier NRG-3v3.

Figure 12: Receiver preamplifier developed and build by NRG

Figure 13 show a sensitivity test of the overall antenna/preamplifier set-up performed above-ground at a recreational area close to the NRG site in Petten, The Netherlands. Next to the peak of the calibration signal at 1133 Hz, only minor interferences of the electric power network are visible at 250 Hz, 400 Hz and 450 Hz. The expected theoretical sensitivity of the set-up, based on the preamplifier performances summarized in Table 3, is between 1 and 2 fT for the frequency range of 1 - 2 kHz. The real measured values are somewhat higher due to several factors:

- Interactions between complex antenna load and the preamplifier;
- Interferences of an unidentified local high-frequency transmitter, probably a "*C2000*" emergency communication system (see also Section 3.1.1);
- Other, mostly natural long-range interferences;
- Artefacts of the discrete Fourier transformation (DFT) applied to generate the frequency spectra

Despite these limiting factors, Figure 13 shows that the set-up developed and build by NRG is capable to detect magnetic field of less than 10 fT in the frequency range of interest.

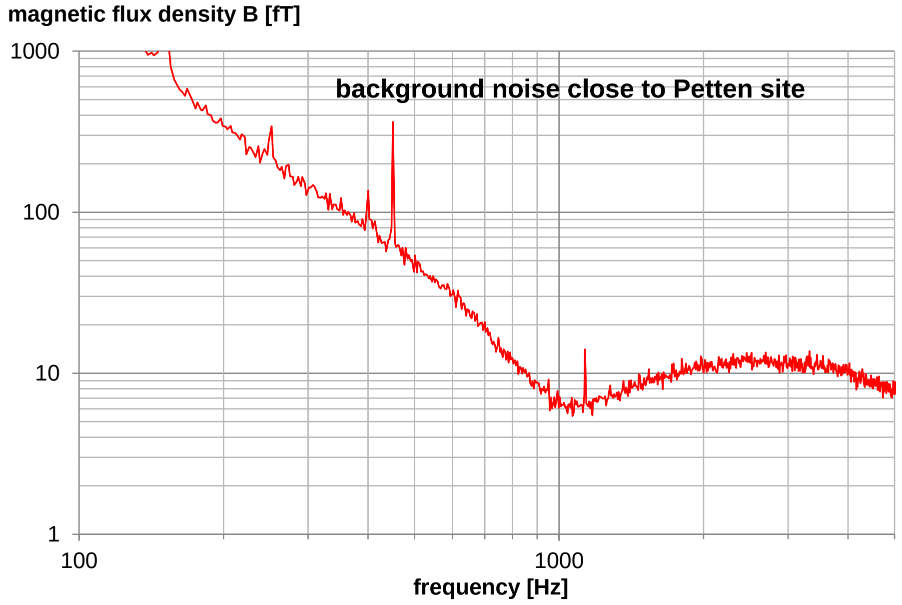

Figure 13: Background noise measured at a recreational area close to the Petten site with loop antenna NRG-4 and preamplifier NRG-3v2. Note that the peak at 1133 Hz is a calibration signal.

2.7 Signal conversion and analysis

Signal conversion was performed with a dual-channel, 24 bit ADC at 192 kHz (input sensitivity see Table 3), and data processing and recording were performed with full frequency- and bit-resolution. Processing/demodulation and analysis of the recorded data were performed by suitable software, partially written by NRG. Signal analysis was performed by DFT, with scalloping loss diminished by the selection of appropriate frequencies [13]. Calibration was performed by measurements of a calibration source at a distance of 3 - 10 m (NRG-1, see Table 1), applying Eq. 3 (see Section 2.9 below).

2.8 Experiments performed at the HADES, Mol

Six measurement campaigns were performed in Mol on 28-10-2010, 26-11-2010, 30-5-2011, 8-8-2012, 10-10-2012, and 9-1-2013. In 2010, the work was focussed on a proof-of-principal of the used set-up, the collection of first data on local background noise pattern and the testing of the several equipment options. The measurement campaign in 2011 and begin 2012 was focussed on optimization of the selected equipment. In 2012, measurements were performed to characterize the frequency-dependent signal attenuation by the geosphere, and in the second half of 2012 and in 2013, experiments for data transmission were performed.

2.9 Additional measurements performed in the Netherlands

Next to the measurements at the HADES, additional measurements were performed in the Netherlands. At the site of NRG in Petten, local noise measurements were performed in order to compare the harmonic spectrum of the local power network interferences in Petten and Mol. In recreational areas close to the NRG site, the sensitivity of the technology was demonstrated in the absence of strong interferences of the on-site electric power network. For these experiments, a coplanar surface-surface configuration was used. The propagation behaviour for this geometry can be described [14] by

$$H_{vertical} = \frac{m_d}{2\pi k^2 r^5}\left[\left(9 + 9ikr - 4k^2r^2 - ik^3r^3\right)e^{-ikr} - 9\right] \qquad \text{Eq. 1}$$

with

$$k = \sqrt{-i\mu\sigma 2\pi f} \qquad \text{Eq. 2}$$

and reformulated for estimating the attenuation, equivalent to Eq. 11 and Eq. 12 in Appendix A:

$$H_{vertical} = \frac{m_d}{2\pi r^3} S_{vertical} \qquad \text{Eq. 3}$$

$$S_{vertical} = \frac{\left(9 + 9ikr - 4k^2r^2 - ik^3r^3\right)e^{-ikr} - 9}{k^2r^2} \qquad \text{Eq. 4}$$

At a distance of 50 to 100 m, the attenuation $S_{vertical}$ can be approximated by a constant value, resulting in a small error for a wide range of conductivities within the frequency range under consideration[5]. Figure 14 shows e.g. the signal attenuation for a frequency of 1500 Hz, resulting in an average value of $S_{vertical}$ of 0.59 with an error of less than 15% at 100 m.

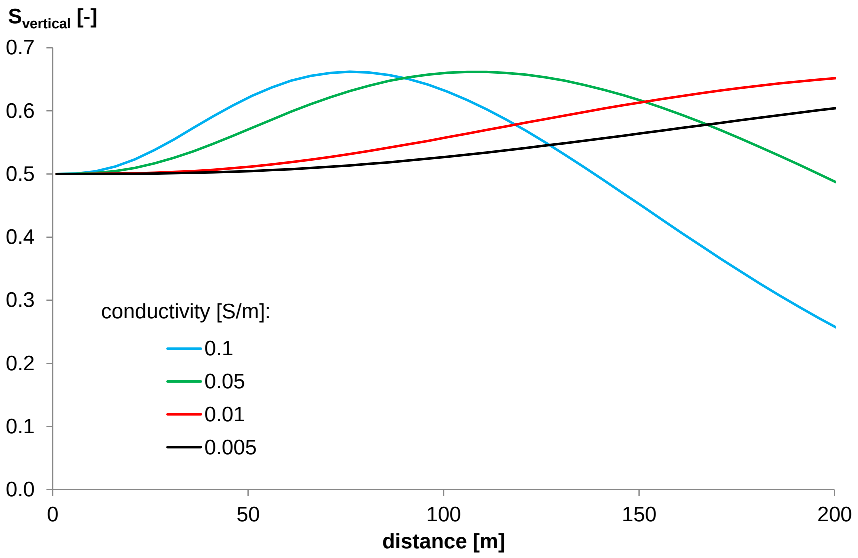

Figure 14: Signal attenuation for a coplanar surface-surface configuration as a function of distance for different conductivities at a frequency of 1500 Hz.

[5] note that correspondingly the conductivity is difficult to obtain by measurements under the given conditions

Eq. 3 is also used for calibration purposes. For this, a magnetic transmitter (loop antenna NRG-1, see Table 1) is located at the surface at 3 or 5 m distance coplanar to receiver antenna. At such small distances, $S_{vertical}$ is close to 0.5 (see Figure 14).

3 Results

3.1 Characterization of signal transmission properties

3.1.1 Location-specific background noise

The measurements performed at Mol were strongly disturbed by the electromagnetic fields emitted by the electric power network on site (and potentially off-site), resulting in a strong interference pattern up to the kHz range. Figure 15 shows an example recorded at Mol above the HADES URL, with peaks of more than 10 pT close to the frequency range of interest. It also shows that the uneven harmonics of the power network are generally stronger than the even harmonics. Additionally, there is a band with increased noise between 2 and 4 kHz, in between the peaks.

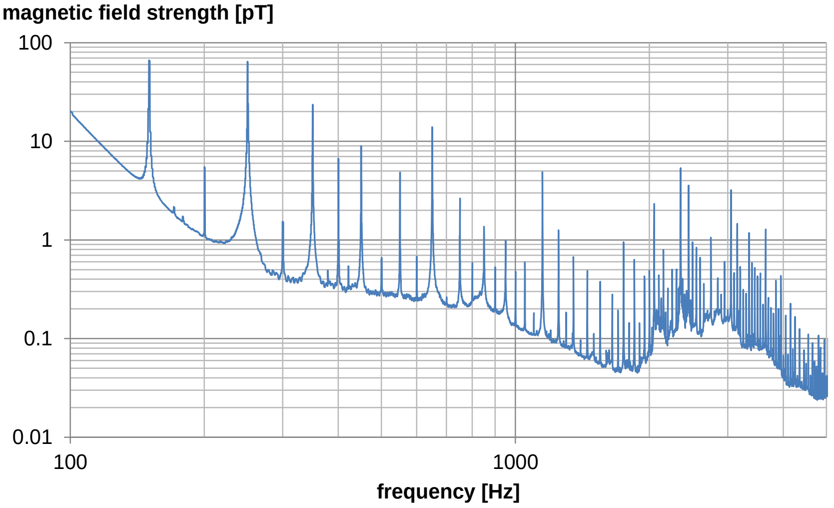

Figure 15: Measured magnetic field strength in Mol at the surface.[6]

Figure 16 shows a more detailed picture of the frequency range considered for data transmission. For data transmission, *transmission channels* can be defined between the peaks, with a bandwidth *BW* of less than 50 Hz. Comparison of Figure 16 and Figure 13 shows, than under the conditions in Mol, the background noise in these transmission channels is about one order of magnitude higher than under less 'noisy' conditions recorded in a more remote area.

[6] note that below 300 Hz, the sensitivity of the preamplifier is (intentionally) low, and values between peaks are not real measured field strength, but preamplifier noise

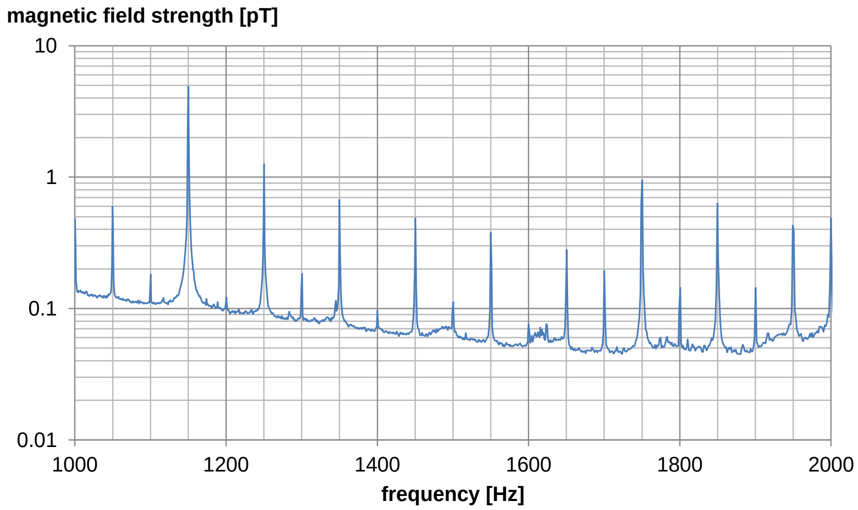

Figure 16: Measured magnetic field strength in Mol at the surface. Note that the small peaks around 1615 Hz belongs to the power spectrum of a modulated data signal.

Relevant differences were found between vertical and radial background noise intensity and pattern. Figure 17 shows an example of the differential noise between the vertical and radial field component. Generally, vertical noise levels appear to be higher than radial, although for some specific frequencies, the radial component is higher. The general pattern depicted in Figure 17 was also observed in other recordings, although some variation between different measurements performed on a day and at different campaigns occurs (data not shown).

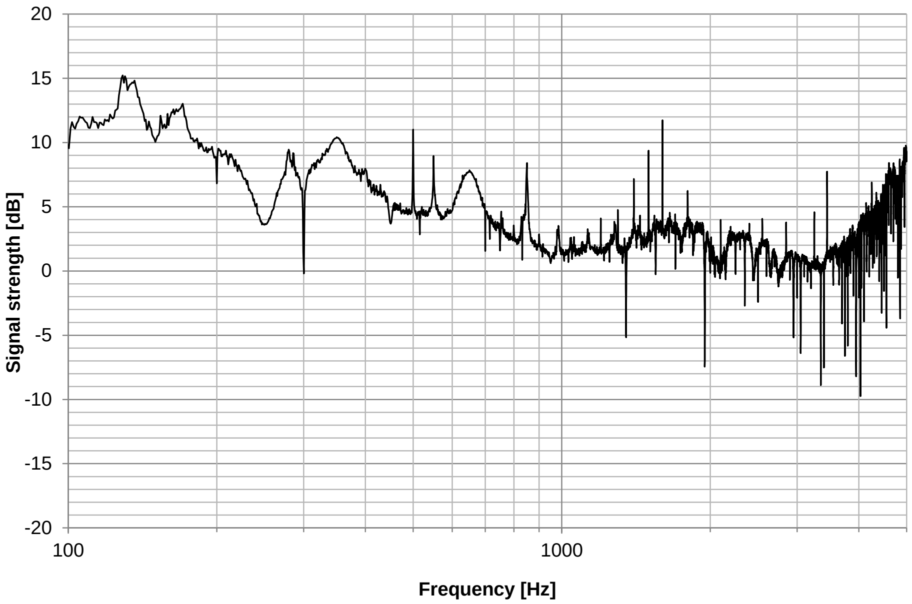

Figure 17: Differential averaged background noise level between vertical and radial field component measured in Mol at the surface.

Analysis of the time-dependent pattern of the interferences by the electric power network shows that these are of rather static nature, although some variations exist on the scale of minutes (e.g. Figure 18) and on longer timescales, e.g. between the different measuring campaigns (Figure 18 vs. Figure 19).

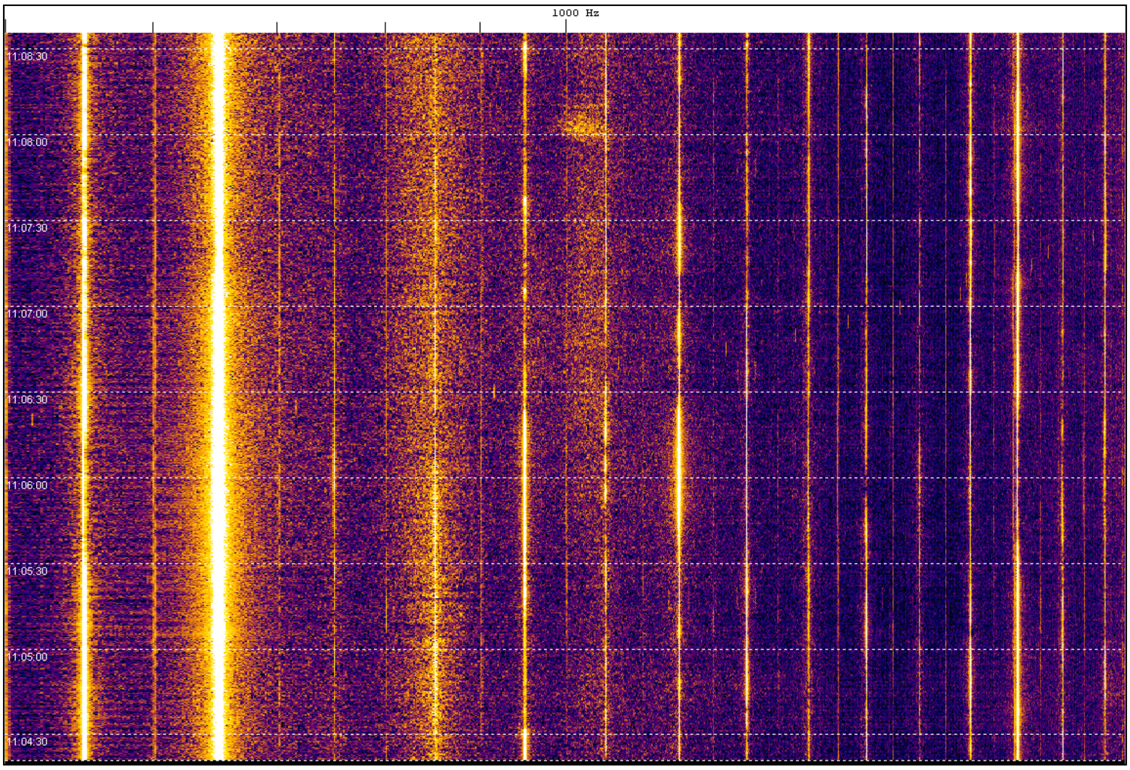

Figure 18: Spectrogram of background noise at the surface in Mol on 8-8-2012. On the horizontal axis the frequency range from 500 Hz to 2 kHz is depicted, on the vertical scale the time axis, with 30 s per division.

Next to the quasi-continuous interference pattern of the power network, also transient interference exits, e.g. by passing cars. Figure 19 shows examples of the interferences of two cars (horizontal yellow lines), resulting in a broad bandwidth disturbance lasting one second or more. Besides, at three frequencies around 900 Hz, repeatedly, pulses of unidentified origin can be found at this particular measurement.

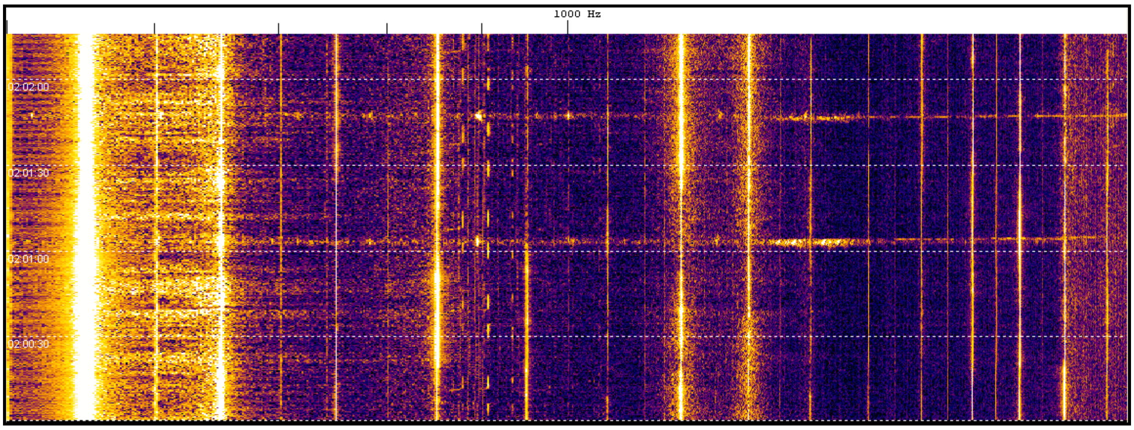

Figure 19: Spectrogram of background noise at the surface in Mol on 30-5-2011. On the horizontal axis the frequency range from 500 Hz to 2 kHz is depicted, on the vertical scale the time axis, with 30 s per division.

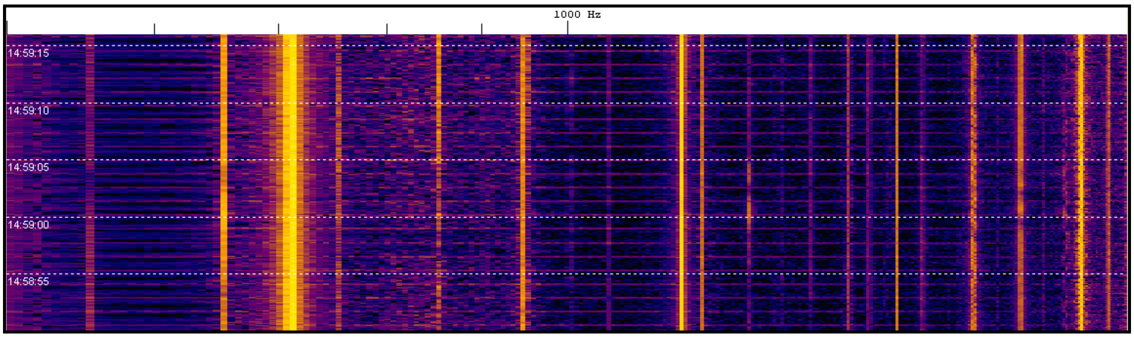

Figure 20: Spectrogram of background noise at the surface in Mol on 10-10-2012. On the horizontal axis the frequency range from 500 Hz to 2 kHz is depicted, on the vertical scale the time axis, with 5 s per division.

With the high sensitivity receiver antenna NRG-4, build at the end of 2011, previously undetected interferences were found. Figure 20 shows horizontal lines in regular intervals of about one second, resulting from short EM pulses (±250 µs) captured by the antenna. The same pattern was found at the Petten site (data not shown) and at a recreational area a few kilometres south of the Petten site (Figure 21). The influence of the equipment (e.g. hard disk drive of the used data logger) could be excluded as well as interferences from GSM phones used for communication. The typical pattern of pulses in a regular interval of 1.0 - 1.4 s could not be attributed to any long-distance source (e.g. civil or military navigation beacons) and is not characteristic to GSM transmitter station protocols [15].

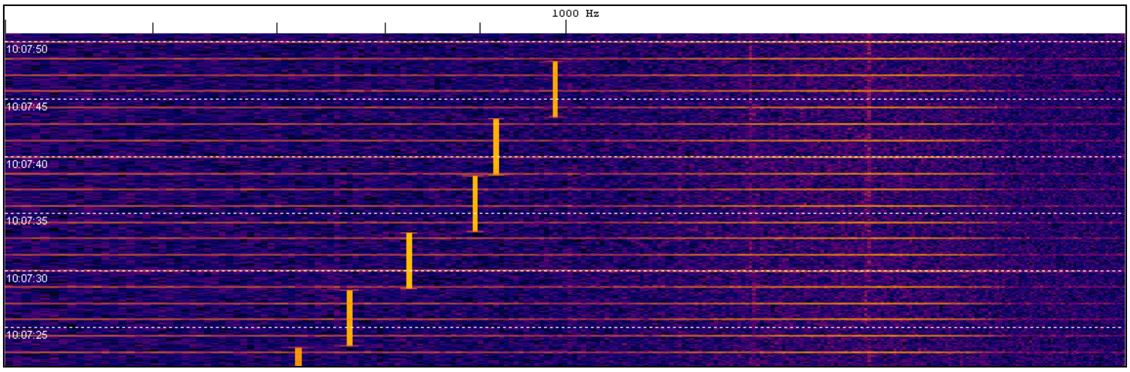

Figure 21: Spectrogram of background noise at the surface in Hargen on 10-11-2011. On the horizontal axis the frequency range from 500 Hz to 2 kHz is depicted, on the vertical scale the time axis, with 5 s per division. Sequential pattern of pulses between 700 and 1000 Hz are transmitted signals.

The national emergency and security communication infrastructure was suspected as one potential source of this interference. This communication infrastructure is based on the *TETRA* technology [16] and known in the Netherlands as "*C2000*" and in Belgium as "*A.S.T.R.I.D.*". *TETRA* transmitter stations have been identified at distances of about 300 m and about 1 km at the recreational area close to the Petten site, and the other two measurement locations, respectively. This is consistent with the magnitude of interferences found at these locations. An additional measurement was performed at a location at a distance of about 4.5 km to the closest *C2000* transmitter station. At this location, no interference by short pulses (as on the other locations) was found (data not shown). Because of the high frequency of these transmitters (390 - 430 MHz), the antennae were positioned in the far-field, and antenna shielding was expected to be only of minor advantage. The use of low-impedance HF-capacitors in parallel with the antenna and connecting cables, in order to remove RF frequencies, did not lower these pulses significantly. However, although these pulses potentially decrease the receivers performance, the short duration of these pulses (<0.03% of time span) had in practice no significant impact on the measurements (see also Figure 13).

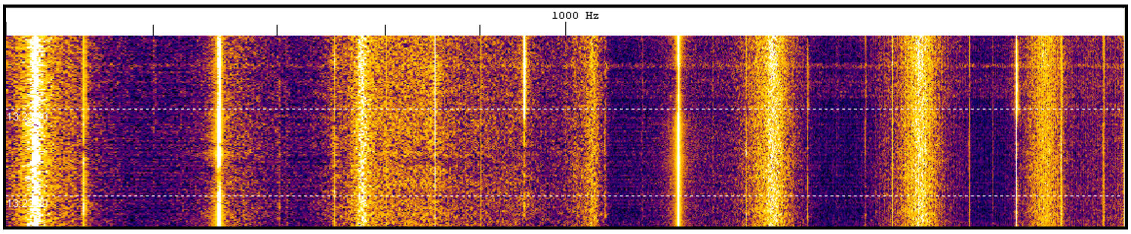

Figure 22: Spectrogram of background noise at the surface in Mol on 10-10-2012. On the horizontal axis the frequency range from 500 Hz to 2 kHz is depicted, on the vertical scale the time axis, with 30 s per division.

Figure 22 shows a specific additional noise pattern registered at Mol on 10-10-2012 only, with broad interference peaks with an interval of about 260 Hz, in addition to the principal pattern of the electric network found in all measurement campaigns at Mol. Although it is difficult to examine due to limited time/frequency resolution provided by techniques as discrete Fourier transformation (DFT), the broad peaks are assumed to be a result of quickly changing frequencies, resulting in a complex frequency and phase behaviour, which it was not possible to eliminate by pre-processing of the data stream prior to demodulation and decoding. Figure 23 shows a 'flat-top'-windowed [13] view on these interferences and depicts more clearly the quickly changing peaks frequencies. In addition to these short term variations over the course of the day, overall variations in frequency and intensity of these additional interferences were also noticed: during the start-up of the experiments on that day (testing, calibration etc.) interferences were present outside the frequency range of interest. It was also noticed that during lunch break interferences disappeared, but experiments could not be performed at that moment.

In conclusion, these particular interferences at the Mol site impaired the measurements carried out on that day, aimed at demonstrating transmission performance at very low energy levels. The source of these interferences could not be identified.

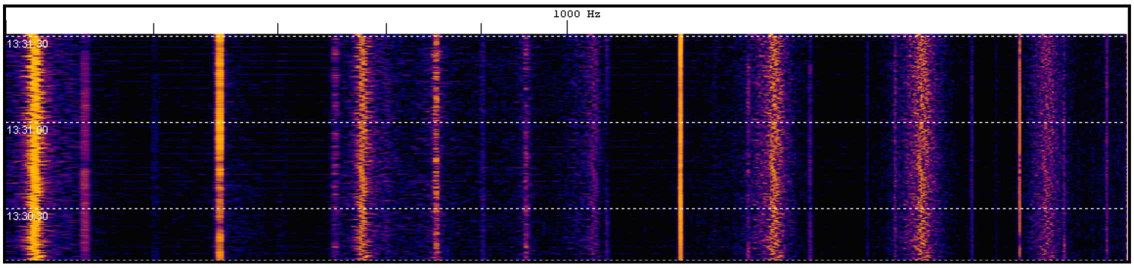

Figure 23: Spectrogram of background noise at the surface in Mol on 10-10-2012. On the horizontal axis the frequency range from 500 Hz to 2 kHz is depicted, on the vertical scale the time axis, with 30 s per division.

Because of the problems described in the previous section, the measurements were repeated on 9-1-2013. However, on that day other interference patterns, not previously detected, were found. In contrast to previous measurements, the interferences were not continuously present, and showed a stable, very specific vertical pattern. Figure 24 shows first undisturbed measurements, followed by the onset of the vertical pattern after 30 seconds, with intervals of about 10 Hz. The long-term averaged spectrum in Figure 25 shows the pattern in more detail (compare with e.g. Figure 16).

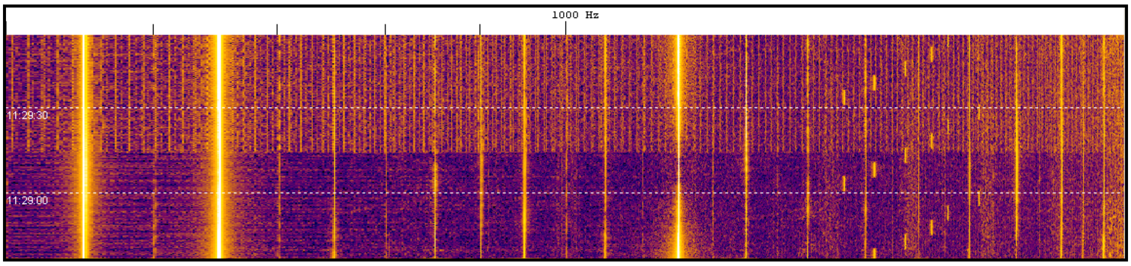

Figure 24: Spectrogram of background noise at the surface in Mol on 9-1-2013. On the horizontal axis the frequency range from 500 Hz to 2 kHz is depicted, on the vertical scale the time axis, with 30 s per division. Sequential pattern of pulses between 1.5 and 1.7 kHz are transmitted signals.

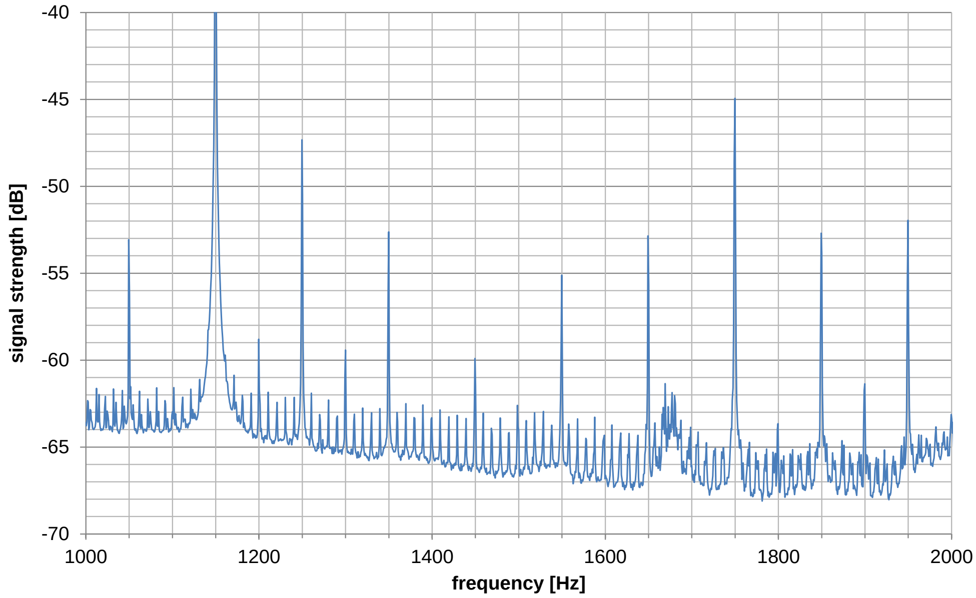

Figure 25: Frequency-dependent background noise at the surface in Mol on 9-1-2013. Note that the small peaks around 1675 Hz belongs to the power spectrum of a modulated data signal.

The observed pattern increases periodically the background noise within the transmission channels of interest by approx. +5 dB, and in one case, a second stepwise increase by +9 dB was found (Figure 26). Unlike in all other measurement campaigns carried out by NRG, on 9-1-2013 it was raining (during all measurements performed on that day). Therefore the presence of drainage pumps in the vicinity of the receiver location was assumed to be a potential source of this very specific interference pattern. However, this could not be confirmed by EURIDICE[7].

These interferences impaired a large part of the measurements performed. An increase in the signal strength could solve the problem only partially, and as consequence the demonstration of data

[7] Jan Verstricht, personal communication

transmission with the lowest possible transmitter energy had to be performed under unfavourable conditions (see Section 3.2).

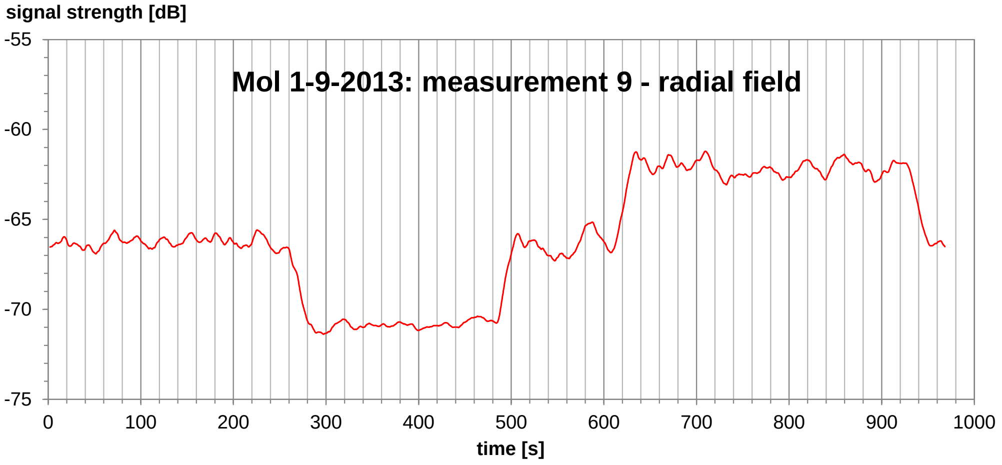

Figure 26: Averaged background noise at selected frequencies at the surface in Mol on 9-1-2013.

In conclusion, the interferences at Mol are found to be relatively high, with few options to avoid them without degrading the principal potential of the set-up used [8]. The measurements were also impaired by the presence of short but large pulses of about 250 µs length. In general, vertical noise levels were found to be larger than radial noise levels in the relevant frequency range, with optimum signal-noise ratios for the radial field component (see next section). Although the very specific, temporary interferences, registered during the last two measurement campaigns, hinder the demonstration of the achievable energy efficiency of the transmission technique under more 'typical' local conditions found during earlier measurements at Mol, sufficient data was collected to support the main objective of this study.

3.1.2 Frequency-dependent signal attenuation

As discussed in Section 2.1 and [8], optimum transmission frequencies were expected for frequencies with wavelength much smaller than the transmission distances, where near-field conditions (Eq. 12 in Appendix A) are no longer applicable. It was assumed that although the direction of the field vector might deviate from what can be estimated by Eq. 12, the overall field strength should be in the same order of magnitude. The measurement of both, vertical and radial field components is therefore essential for quantification of the overall field strength at different frequencies.

Besides the theoretical uncertainties arising from the available approximation functions applied, there are also some uncertainties with respect to the experimental quantification of the propagation behaviour:

- The electrical conductivity of the transmission path is approximated, and the conductivity below the HADES is only partially known;
- The (horizontal) stratification of the transmission path is not accounted for;

[8] I.e. a set-up is possible that may perform better under the particular condition present in Mol, but this would perform less under more favourable conditions

- In view of large differences in conductivity expected between the saturated and unsaturated layers, it must be assumed that the receiver antenna is not precisely located at the interface conducting/non-conducting medium (i.e. groundwater table), but about 1 - 1.5 m above;
- The effect of the presence of magnetic permeable materials in the HADES on the field vector is difficult to assess;
- The quantification of (small) signals in a complex spectrum (see previous section) by DFT has a limited precision;
- In the frequency range where significant attenuation is expected to be measurable, background noise is extremely high and variable (>100fT on average even between the harmonics of the power network; see Figure 15).

Figure 27 shows the magnetic field strength of the radial field component as a percentage of the vertical field component. The contribution of the radial component increases with the frequency, as expected. This is consistent with expected magnetic field propagation behaviour in the extended near-field. Also the sum of both radial and vertical magnetic field components is within expectation, as discussed below. However, the overall contribution of the radial field is much larger as can be expected from Eq. 12 (Appendix A). Also, the receiver antenna is positioned about 10 m off-axis due to practical reasons (the presence of a connecting road directly on top of the HADES gallery). Additionally, the receiver antenna is positioned above the interface between conducting/non-conducting medium, which can be considered on top of the water table.

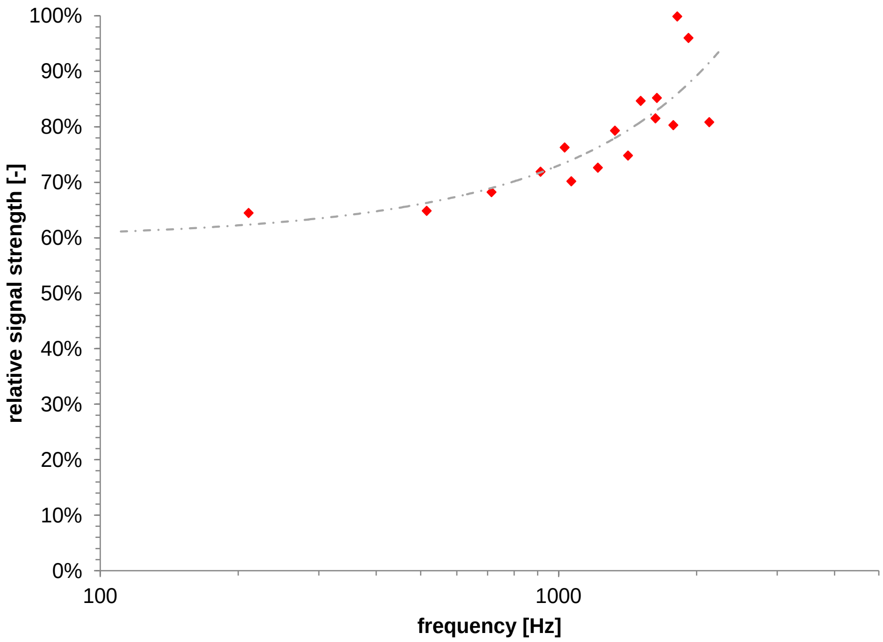

Figure 27: Measured radial signal strength, relative to the vertical field.

Figure 28 shows the results of signal transmission measurements carried out at a number of frequencies between 200 Hz and 5 kHz. The overall field strength results from measurements of the vertical and radial field components at the surface. Below 2.3 kHz, transmitted signals could be clearly identified, with standard deviations of the repeated measurements below 2 dB for most cases. As result of the increased (average) noise level found for frequencies > 2 kHz (Figure 28), above 2.3 kHz it was increasingly difficult to distinguish between incidental bursts and 'true' signal reception. This is consistent with the higher standard deviations found in repeated measurement. However, no algorithms could be found that could enable signals to be distinguished, in a statistical significant manner, from incidental noise bursts above 2.3 kHz. Thus, for frequencies above 2.3 kHz, the signal strengths depicted in Figure 28 can either represent received signals, noise, or a combination of both.

The recorded signal strength is generally in line with values calculated on basis of the model description of the set-up used (see [8]) and the averaged conductivity derived from Figure 4. Additionally, the electrical conductivity value was fitted with the measured values, resulting in a conductivity value of 50 mS/m (Figure 29). Given the uncertainties of the experimental set-up and the approximation function used and discussed previously, it is unclear whether the deviations above 2.3 kHz must be attributed to the derived conductivity value, or it is a result of the extrapolation of Eq. 12 beyond near-field. However, when comparing all outcomes, overall resulting uncertainties are limited to a factor of two.

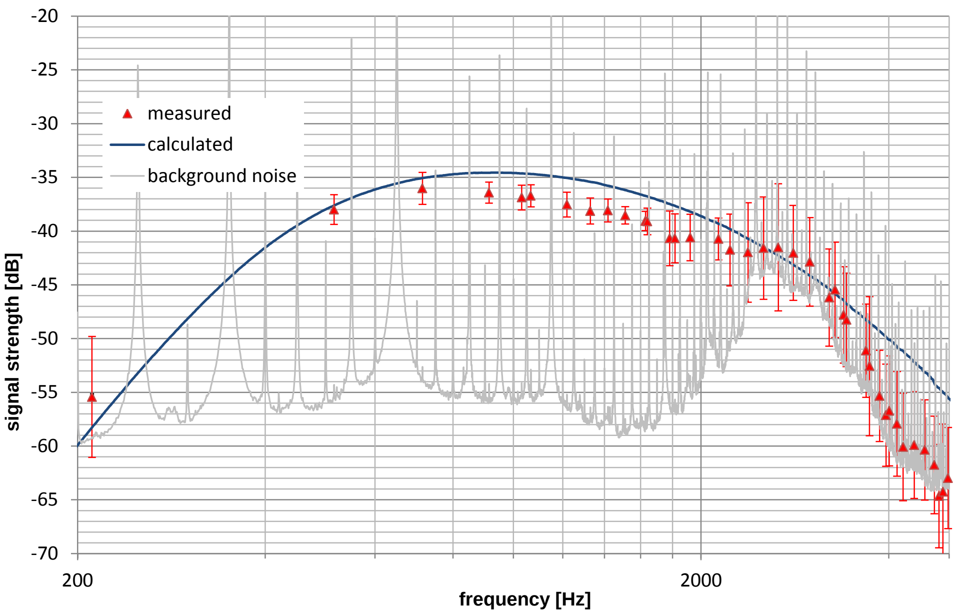

Figure 28: Measured and calculated signals strengths, and averaged background noise level recorded at the surface in Mol on 8-8-2012 (σ = 33 mS/m, r = 225 m). Error bars represents the measured standard deviation.

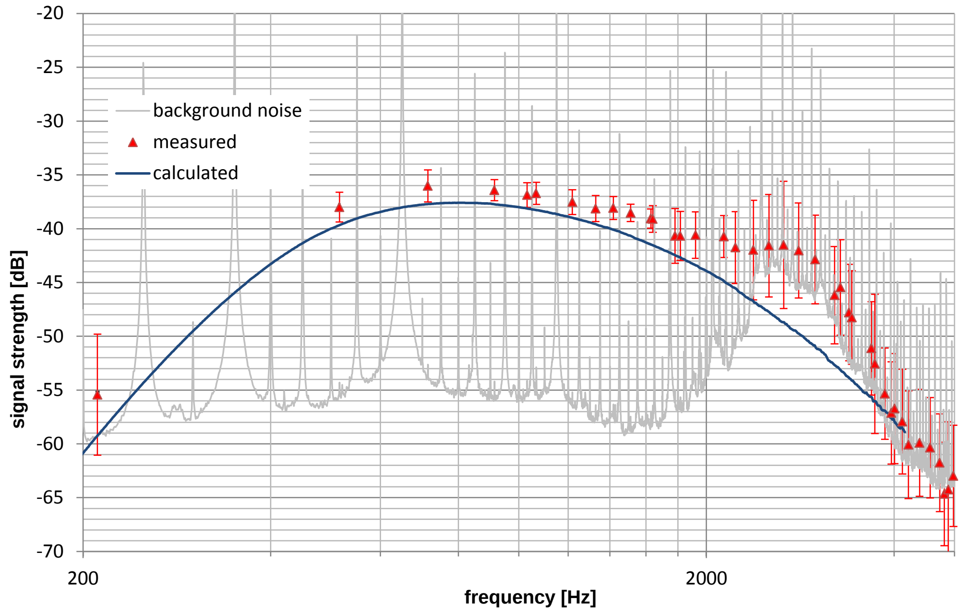

Figure 29: Measured and calculated signals strengths, and averaged background noise level recorded at the surface in Mol on 8-8-2012 (σ = 50 mS/m, r = 225 m). Error bars represents the measured standard deviation.

Figure 30 depicts the signal attenuation by interactions with the geological medium only (i.e. not related to the distance) for the measured values and the model calculations. Generally, signals are attenuated weakly at low frequencies, about a factor of ten between 2 and 3 kHz and more than linear with frequency above 2 kHz (i.e. faster than is compensated by increasing antenna sensitivity).

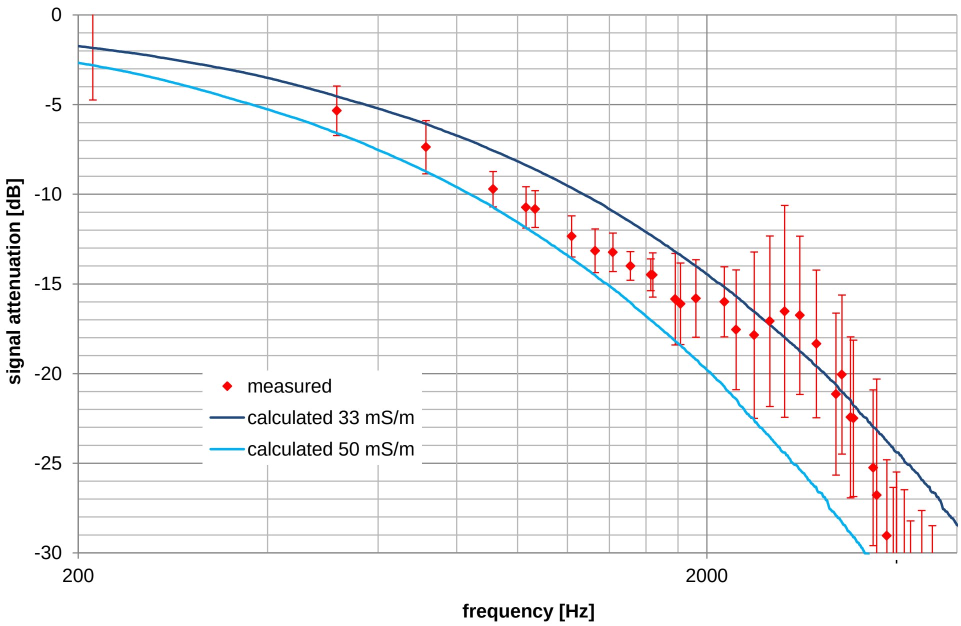

Figure 30: Measured and calculated signal attenuation by the geological medium (r = 225 m) between 200 Hz and 5 kHz. Error bars represents the measured standard deviation. Note that measured values above 2.3 kHz may also result from background noise.

In conclusion, although the radial field component was found to be unexpectedly large compared to the vertical component, the overall field strength was generally in line with what was expected on basis of the near-field propagation behaviour. The results of the signal transmission experiments give a good indication of the propagation behaviour beyond the near-field, and support the selection of suitable channels for data transmission. From Figure 28 it can already be derived that the largest signal-to-noise ratios can be expected in the range of 1.0 to 1.7 kHz. In the next section, the selection of suitable data transmission channels will be presented in more detail.

3.1.3 Channel identification

In order to identify suitable channels for data transmission, a detailed investigation of the background noise pattern was carried out. Figure 31 shows an example of vertical and radial noise in the range of 1.0 and 1.7 kHz, which was considered the most suitable frequency range for data transmission on basis of the noise measurements and the propagation behaviour discussed in the previous sections. Generally, it can be noted that when selecting most suitable channels for data transmission within a given range, higher frequencies should be favoured, because a) antenna sensitivity is linear related to the frequency, and b) at higher frequencies, a higher bandwidth can be achieved (see also [8]).

For the particular situation at Mol, it has already been shown that the radial noise levels are smaller than the vertical noise level (Figure 17). With some variations between different measurements, differences in noise level for the considered transmission channels were generally ranging between 2 and 8 dB, with larger differences at higher frequencies (e.g. Figure 31). In comparison, radial signal strength was found to be 70 - 85% of the vertical signal strength in the considered range (see Figure 27), equivalent to -3.1 to -1.4 dB. Thus, for most frequencies, the signal-to-noise ratio of the radial field is larger than for the vertical.

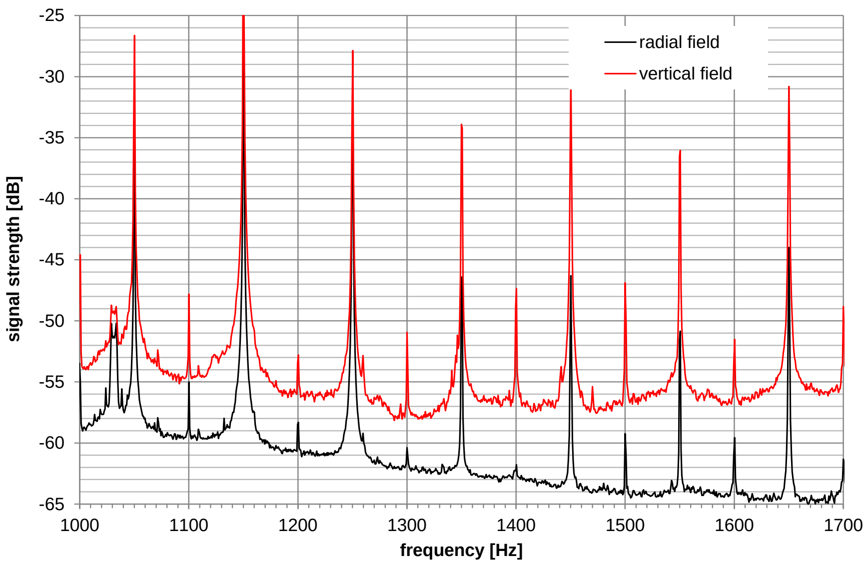

Figure 31: Averaged radial and vertical background noise level measured in Mol at the surface. Note that the small peaks around 1033 Hz belongs to the power spectrum of a modulated data signal.

When investigating individual channels, next to the harmonic spectrum of the electricity network, eventually, additional smaller individual peaks were found (Figure 31). These peaks are potentially relevant because they may significantly interfere with specific combinations of data modulation and symbol rates. Figure 31 also shows incidentally that even harmonics of the electricity network are low enough to allow the definition of transmission channels with a bandwidth larger than 50 Hz (e.g. at 1400 Hz, radial field). However, comparison of all aggregated data shows that these smaller harmonic peaks can vary in intensity during the day, reflecting difference in energy use of the surrounding facilities.

In order to analyse channel behaviour in more detail, additional tools were developed that allow cumulative frequency distributions (cfd's) of the DFT bin's in the area of interest to be computed. Figure 32 and Figure 33 show examples of a favourable and a less favourable cfd's, obtained for two different frequency ranges. The channel noise in Figure 33 exceeds 60 dB only for 10% of the sampled time intervals, whereas in the channel in Figure 32 this is the case in 26% of the intervals. For data transmission this is potentially more significant than the rather small differences in average noise level (less than 2 dB / 20%). It should be noted that although the cfd analysis allows identification of less suitable channels, cfd's outcomes could not be directly related to the channel performance. This is due to the temporal variability of some interferences and lack of sufficiently long undisturbed measurements, that are required to allow an accurate statistical analysis of data transmission performance (see Section 3.2). Thus, although cfd's provides valuable information for the selection of channel under the specific conditions present in Mol, no further quantitative evaluations to link cfd's with transmission results were performed here.

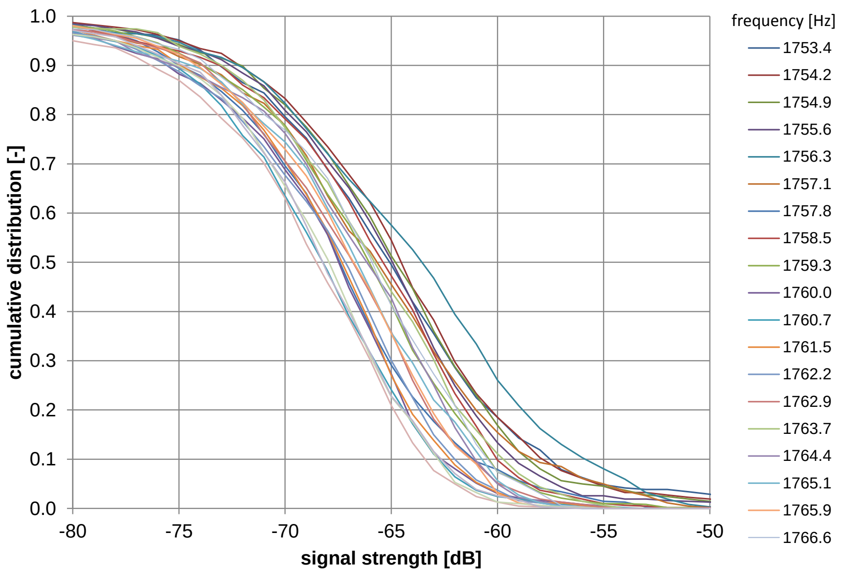

Figure 32: Cumulative distribution of background noise level at different frequencies.

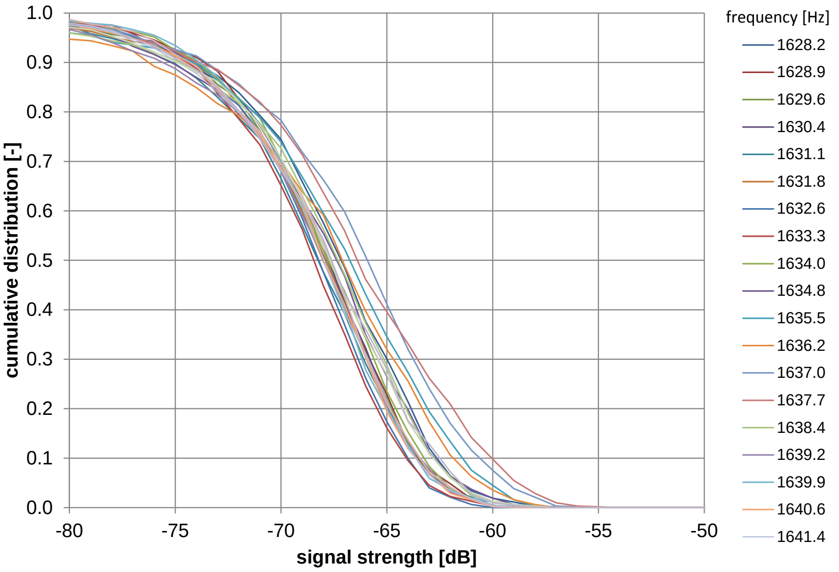

Figure 33: Cumulative distribution of background noise level at different frequencies.

Based on the analyses presented in this section, several data transmission channels have been identified between 1450 Hz and 1650 Hz. The data transmission experiments and their results will be discussed in the next chapter.

3.2 Demonstration of data transmission

3.2.1 Used modes, transmission speeds and channels

On 8-8-2012, 10-10-2012, and 9-1-2013, data transmission experiments were performed at the HADES. On 8-8-2012, only a limited '*proof-of-principle*' study was carried out, using the large bandwidth transmitter antenna NRG-2. For the particular (small bandwidth) application a more energy-efficient antenna was constructed (NRG-3, see Table 2) and used during the experiments performed on 10-10-2012. The same antenna design was used on 9-1-2013, and to avoid potential problems as those emerged during the experiments on 8-8-2012 (see Section 3.1.1), a switchboard was built that enabled the antenna NRG-3 to be tuned to several transmission channels, distributed over a larger frequency range.

As "data", in all experiments a text string was used that was coded with the lossless *Varicode* compression scheme [17]. The text string contains information on the selected transmission frequency, symbol rate and signal level. The text strings were transmitted repeatedly, and the bit error rate (BER) was calculated by dividing the number of received errors by the number of total bits transmitted. In case of a BER>1%, the transmission was assumed to be too scrambled for practical purposes (see also Eq. 15, Annex A in [8]), and no further quantification of the BER was performed.

For the modulation of data, the so-called 'phase-shift-keying' (PSK) modulation scheme has been selected, due to its favourable energy-efficiency [8]. Besides, this method was assumed to be more 'robust' with respect to the specific background noise pattern present in Mol (i.e. presence of large interference peaks with invariable phase behaviour and incidental short energy burst). Although PSK can be implemented as *m-ary* PSK, with *m* the number of states of each symbol, the experiments performed by NRG were limited to binary phase shift keying (BPSK, with two different states). The main advantage of the use of *m-ary* methods with *m*>2 is a larger achievable bandwidth (not of primary relevance for the application in post-closure monitoring) against minor improvements in energy efficiency, if any at all. However, the *m-ary* method leads to an increased complexity of the method performance evaluation (i.e. variable inter-symbol distances, partially optimized by complex data coding methods).

It was difficult to estimate in advance, how local interferences in Mol would affect data transmission performances, because local interferences are not behaving like random, Gaussian noise (see previous section and Section 3.1.1). Besides, spectrum analysis techniques like DFT have a limited time-frequency resolution, potentially overlooking short spikes or burst-like patterns. Based on the analyses described in the previous section, several transmission channels were selected on basis of their signal-noise ratio, ranging from 1.4 to 1.7 kHz (1.0 - 1.1 kHz for the first 'proof-of-principles').

Because of the local interference pattern, the data rates selected to be tested were chosen to cover a large range, from 3 sym/s to 30 sym/s, in order to anticipate large temporal variations of the noise spectrum at some frequencies. In general terms, a transmission channel can be envisaged as a homogeneous part of the spectrum with equally distributed (random) noise, i.e. in case of the HADES experiments, expected channel bandwidth is less than 50 sym/s due to the presence of the strong harmonics of the power network. Accounting for numerical effects of the computational, discrete processing of the data, and potential non-linearity of the transmission chain, a data rate of 30 sym/s was assumed as a reliable maximum data rate that would fit in the harmonic spectrum found at Mol[9].

However, closer analysis of the specific power spectrum of the BPSK-modulated data signal showed that some frequencies are not required for the reconstruction of the original data. It was postulated that when transmission frequency and data rate is carefully matched to the existing interferences, data rates above 50 sym/s may be achieved. In order to test this hypothesis, additional experiments were performed on 9-1-2013 with data rates of 60, 90 and 100 sym/s. Besides the expected higher energy efficiency, the higher data rates allow an easier comparison of modulation method performances in a less 'noisy' location (see Section 4.1)

3.2.2 Results of data transmission experiments performed at the HADES URL

On three visits to Mol, data transmission experiments were performed. Two example of the received text strings are depicted below (errors marked in red)[10]:

Data-stream 5, vertical antenna, 1031.3 Hz, 5 sym/s, 0 dB

```
BPSK 5s  /s 0dB 1031.3Hz
BPSK 5sym/s 0dB 1031.3Hz
BPSK 5sym/s 0dB 1031.3Hz
```

[9] although higher data-rates might be achieved without loss of performance (e.g. 40 sym/s), this was not investigated by NRG, because collecting sufficient data to give statically sound evidence for a better performance of e.g. 40 sym/s against 30 sym/s would need too much time (see also Section 2.1)

[10] note that in *Varicode*, letters are coded with variable number of bits

```
BPSK 5sym/s 0dB 1031.3Hz
BPSti 5sym/s 0dB 1031.3Hz
BPSK 5sym/s 0dB 1031.3Hz
BPSKtgsym/s 0dB 1031.3Hz
```

-> 1134 bit, 5 errors: BER = 0.4%

Data-stream 6, vertical antenna, 1031.3 Hz, 3 sym/s, 0 dB

```
     3sym/s 0dB 1031.3Hz
BPSK 3sym/s áB 1031.3=z
BPSK 3sym/s 0dB 1031.3Hz
BPSK 3sym/s 0dB 1031.3Hz
BPSK 3sym/s {12}iB 1031.3Hz
BPSK 3sym/s 0dB 1031.3Hz
BPSK 3sym/s 0dB 1031.3Hz
BPSK 3sym/s 0dB 1031.
```

-> 1241 bit, 5 errors: BER = 0.4%

On 8-8-2012, as 'proof-of-principle', three data transmission experiments were performed, with a conservative data rate ranging from 3 to 10 sym/s. The outcome of the data transmission experiments (Table 4) demonstrated that data transmission is possible with BERs of less than 0.4%[11]. Analysis of the results in detail gave good indications on general features/limitations of data transmission under the conditions present in Mol and the expected performances that might be realised. The outcomes were used to design an optimized set-up of the transmitter antenna and receiver design used solely for data transmission experiments for the next visit to Mol.

Table 4: Results of selected data-transmission experiment performed at 8-8-2012

Record number	Frequency [Hz]	Data rate [sym/s]	Signal level [dB]	BER* [%]
5	1031.3	5	0	0.4
6	1031.3	3 10	0 0	0.4 >1
7	1066.4	3 5 10	0 0 0	0.0 0.1 >1
8	1031.3	3	-6 & -12	>1

* indicative value

On 10-10-2012, a second set of data transmission experiments was performed using the transmitter antenna NRG-3 (Table 1). However, the expected performance could not be demonstrated on that day, because a new, previously undetected broad bandwidth interference disturbed the reception of transmitted data in all four channels defined for the experiments (see Section 3.1.1). The main

[11] note these values are indicative because the number of transmitted bits was too small to allow a quantitative evaluation (1-2kb)

objective on 10-10-2012 was to demonstrate data transmission at the lowest possible energy level. The real-time processing on location only delivered a first, conservative estimation of transmission performance, therefore it was decided not to increase the transmission energy used for the experiments and to evaluates afterwards whether the transmission performance can be improved by pre-processing of the data stream prior to demodulation and decoding. Consequently, only one of the conducted experiments resulted in a BER < 1% (Table 5). It was therefore decided to repeat the measurements on an additional visit to Mol.

Table 5: Results of selected data-transmission experiment performed at 10-10-2012

Record number	Frequency [Hz]	Data rate [sym/s]	Signal level [dB]	Energy [Ws/bit]	BER* [%]
1	1627.1	10	0 -3	2.6 1.3	>1 >1
2	1476.9	10	0	3.6	>1
3	1488.4	20	0	1.8	>1
4	1613.5	20	0	1.3	>1
5	1613.5	20	0	1.1	>1
6	1613.5	20	0 -2	1.3 1.0	>1 >1
7	1613.5	20	-2 -4	1.0 0.6	0.5 >1
8	1613.5	20	-4 -6	0.6 0.4	>1 >1

* indicative value

On 9-1-2013, the data transmission experiments at the HADES were repeated, with the set-up partially adapted based on previous experience. As discussed in Section 3.1.1, on this day (part of) the measurements were disturbed by new, previously not recorded discrete interference, most likely produced by drainage pumps. The time intervals at which this interference was present was quantified for each record by signal analysis (see for an example Figure 26). The analysis of the data transmission performance was conducted only for the time intervals where the interference was absent[12], resulting in the BER's summarized in Table 6.

Despite the unfavourable conditions, data transmission with symbol rates up to 100 sym/s could be realised. The results in Table 6 with BER<1% are based on about 25'000 transmitted bits.

[12] note that for record 14 (10 sym/s) time intervals could be used in which the interferences were present

Table 6: Results of selected data-transmission experiment performed at 9-1-2013

Record number	Frequency [Hz]	Data rate [sym/s]	Signal level [dB]	Energy [Ws/bit]	BER* [%]
3	1523.8	30	0	1.1	>1
4	1573.8	30	0	0.9	>1
6	1675.0	25	0	1.3	0.4
7	1523.8	30	0	4.2	0.7
8	1523.8	30	0 -3 -6 -9 -12	4.2 2.1 1.1 0.5 0.3	0.4 0.5 >1 >1 >1
9	1573.8	30	0 -3 -6	4.2 2.1 1.1	>1 >1 >1
10	1573.8	30	0 -3 -6	7.3 3.7 1.8	0 0.06 0.06
11	1613.5	90	0	2.2	>1
11a	1613.5	90	0	1.9	0.4
12	1606.7	60	0	3.3	0.06
13	1606.7	100	0	2.0	0.2
14	1627.2	10	0 -3 -6 -9 -12	19.0 9.5 4.8 2.4 1.2	0 0 0.2 0.2 >1

* indicative value

In conclusion, the experimental work performed by NRG at the HADES URL demonstrated the ability to transmit monitoring data wirelessly from a deep underground disposal facility to the surface on several occasions and with different data rates up to 100 sym/s. Bit error rates of 0.1% and below were realized, although the total number of data is rather small (±25'000 bit) to allow a proper quantitative evaluation of the method performance. The presence of strong interferences on the surface and activities on-site (e.g. passing cars, shaft lift, construction works) affected the quality of the data and meant that a proper statistical evaluation of data transmission experiments was not possible.

3.2.3 Results of additional data transmission experiments performed in the Netherlands

By additional surface-surface experiments performed in a remote area close to the Petten site, it could be demonstrated that principal sensitivity of the setup is high enough to transmit data with less than 10 µWs/bit over a distance of 50 m (see Section 2.9). Table 7 summarizes the energy used and the bit error rates achieved in these experiments (compare also with Table 6).

Table 7: Energy use and bit error rate (BER) in coplanar configuration measured in a recreational area close to the Petten site (transmitter antenna NRG-3, transmission distance *r* = 50 m)

transmission mode	1606.7 Hz 100 sym/s	1523.8 Hz - 30 sym/s				
		0 dB	-3 dB	-6 dB	-9 dB	-12 dB
Energy [mWs/bit]	0.013	0.044	0.022	0.011	0.006	0.003
BER [%]*	0.006	0	0.03	0	0	0.8

* indicative values based on 26'000 transmitted bits

The results can be extrapolated in order to estimate the energy use for the transmission of data from the HADES to the surface in case of less strong local interferences. Correction for the larger transmission distance and the differences in signal transmission in the coplanar configuration used for the surface-surface experiments, and the coaxial configuration in case of the HADES can easily be performed by applying Eq. 3 and Eq. 10. Signal attenuation due to interactions of the field with the geological medium in case of the HADES can be estimated from measured values in Figure 30 (compare also with Figure 14). The results of this extrapolation are summarized in Table 8 and show that under less unfavourable conditions at the Mol site, data transmission might be achieved with less than 10 mWs/bit, even with small transmitter antennas as used in the HADES ($r < 2$ m).

Table 8: Extrapolated energy use for data transmission from the HADES URL to the surface in case of weaker local interferences from power network, based on measurement in a recreational area close to the Petten site in coplanar configuration, and signal attenuation measurements performed at the HADES URL

transmission mode	1606.7 Hz 100 sym/s	1523.8 Hz - 30 sym/s				
		0 dB	-3 dB	-6 dB	-9 dB	-12 dB
Energy [mWs/bit]	3.2	10.8	5.4	2.7	1.35	0.67

4 Analysis of energy need

The energy required to transmit data from a deep geological disposal to the surface by the low-frequency magneto-induction technique developed by NRG can be estimated by applying the equations and considerations discussed in [8]. The main objective of the work performed in WP3.4 was to demonstrate the applicability of the framework developed in [8] under realistic conditions. As discussed in Section 3.1.2, it was also found necessary to give experimental support for the theoretical considerations on the propagation behaviour of the geosphere. While it was found that the theoretical consideration are consistent with the experimental results, the specific boundary conditions at the HADES discussed in Section 2.1 made it necessary to perform some additional analyses in order to estimate the achievable energy efficiency of the developed technique in the application case.

In the next sections, the outcome of the demonstration work at the HADES was compared with the outcome of WP2.3, presented in [8], and estimations of energy efficiency of the developed technique for "real" disposal situations were performed.

4.1 Demonstrated and optimum energy efficiency

Generally, the overall signal transmission behaviour is found to be in line with what is expected on the basis of the WP2.3 report [8]: Figure 28 shows that the received signal strength is close to the expected values. The optimum signal transmission frequency could not be supported experimentally, partially because of the high noise level present at frequencies above 1.7 kHz, and partially because of the small influence of the frequency close to the optimum: Figure 5 shows that transmission frequency can deviate from the optimum frequency by about ±0.5 kHz with a 'penalty' of less than 20%. Extrapolation of additional surface-surface measurements (Section 3.2.3) provided evidence that under less unfavourable conditions assumed for the Mol site, data transmission from the HADES to the earth's surface with only a few mWs/bit can be feasible, further underlining the analyses performed in [8].

Assuming all noise and interferences present as average white Gaussian noise, the relation between energy level and transmission performance (bit error rate) can be calculated by

$$BER\ [-] \approx \frac{1}{2} erfc \sqrt{\frac{E_b}{N_0}} \qquad \text{Eq. 5}$$

with E_b the energy level per bit and N_0 the power noise spectral density [8]. Although detailed analyses of the BER are difficult due to the low data rates and experimental circumstances as discussed in the previous sections, Figure 34 showed that the best performances demonstrated at the HADES are generally in line with Eq. 5. In a few cases, performance seemed to be better than expected (i.e. points are below the line). However, as noted before, the number of data bits transmitted was too low to allow statistical analyses, and it can be noted that in four cases the BER even equals zero (not shown because of the *log-log* scale of Figure 34).

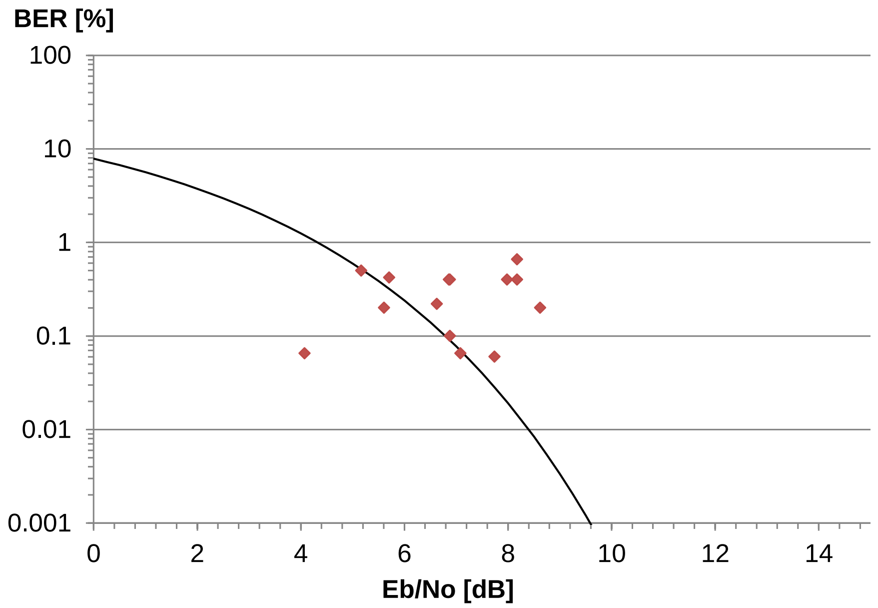

Figure 34: Measured (red diamonds) and calculated (black line) bit error rates (BER) as function of the signal strength divided by the background noise. Note that BER values are indicative due to the limited number of data transmitted.

Overall, the most efficient data transmission from the HADES to the surface could be achieved with an energy of about 1 Ws/bit, which is almost a factor 2 higher than estimated, but still a quite accurate result when considering the uncertainties discussed. This finding provides some confidence in the quantitative analyses performed in WP2.3 [8]. In the next section, some extrapolations are performed in order to judge the energy needs in future application cases.

4.2 Extrapolation of energy need to selected disposal designs

For the planning and set-up of a data transmission chain, a number of properties and features must be taken into account. Since components interact with each other in a complex way [8], a simplified straightforward method for a general outline of all components is discussed in this section, and two application examples are given. Generally, a four-step scheme can be followed:

1. Estimate optimum transmission frequency;
2. Define transmitter antenna properties and estimate maximum bandwidth;
3. Estimate required field strength at the surface;
4. Estimate power to generate the required magnetic moment.

In the following paragraphs, two example calculations are presented: one for the generic Dutch disposal concept in Boom Clay, and one for the generic Dutch concept in rock salt.

4.2.1 Case 1: generic Dutch disposal concept in Boom Clay

In a first step, the optimum transmission frequency for this situation can be estimated, considering the transmission distance and the (averaged) electrical conductivity of the transmission path. In case of the generic Dutch disposal concept in Boom Clay [7], the transmission distance is 500 m, and the electrical conductivity is assumed to be comparable to the values found at the HADES (Figure 4, see also Figure 30). By making use of Eq. 37 and Eq. 39 in Annex A in [8], two approaches can be followed to estimate the optimum transmission frequencies:

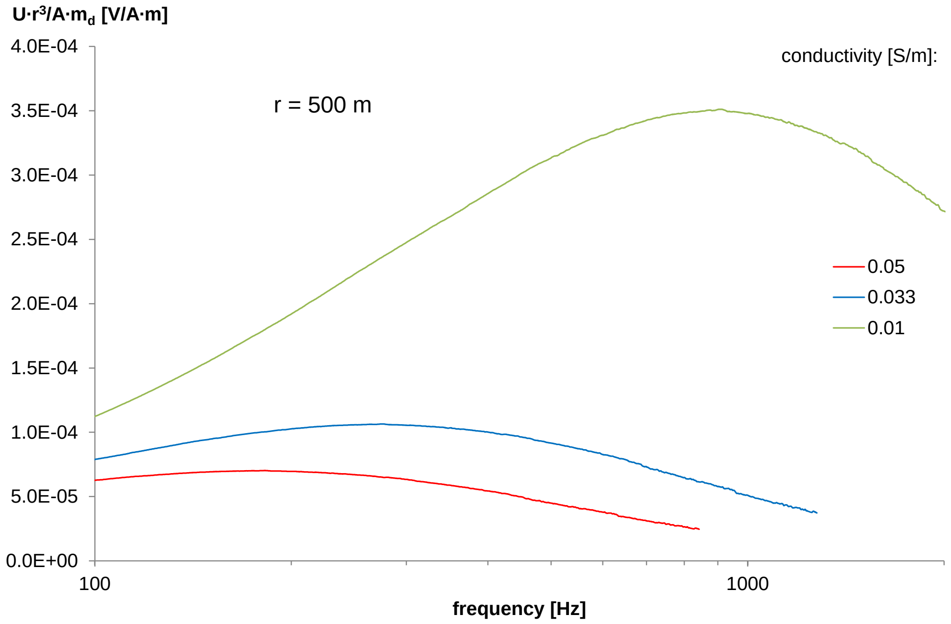

Figure 35: Transfer function for magnetic field propagation through a conducting medium and reception by a loop antenna for a transmission distance of 500 m and electrical conductivities between 0.01 and 0.05 S/m

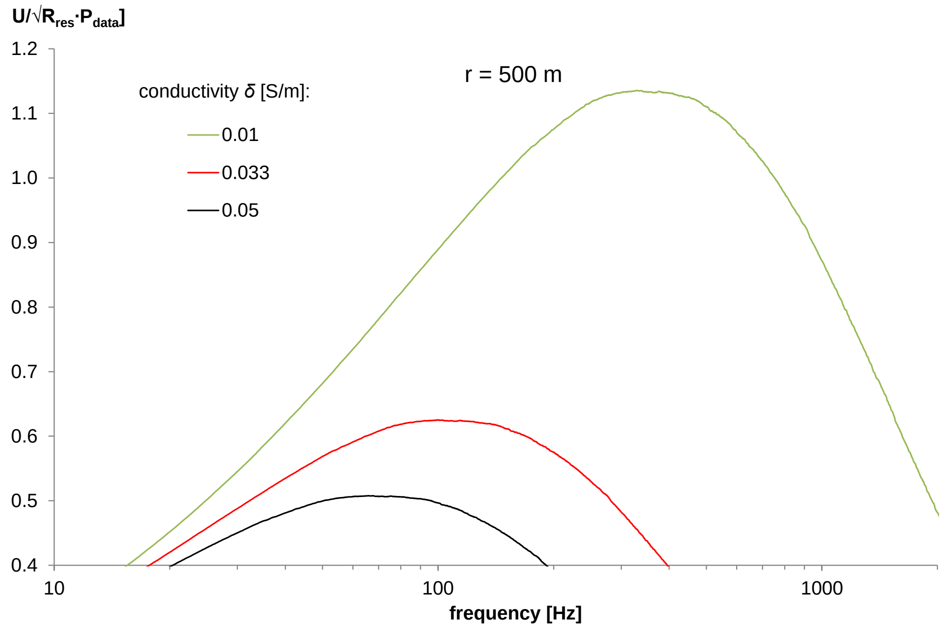

Figure 36: Transfer function for data transmission through a conducting medium for a resonant transmitter antenna, a transmission distance of 500 m and electrical conductivities between 0.01 and 0.05 S/m

Figure 35 and Figure 36 show that optimum transmission frequencies for the generic Dutch disposal at 500 m depth are much lower compared to those for the 225 m distance used in the HADES experiments. For the conductivity range of 33 to 50mS/m, optimum frequencies are around 100 Hz, and much higher frequencies might be used at conductivities of 10 mS/m or lower. For further analysis, transmission frequencies of 75, 150 and 250 Hz were selected.

In a second step, the transmitter antenna properties are defined. In [8] it was argued that the optimum transmitter antenna radius will be slightly smaller than the transmission distance. In case of the generic Dutch disposal concept in Boom Clay, three antenna radii were considered: 500 m, 250 m and 125 m. Antenna inductivity can be estimated by Eq. 9. Since this equation is only valid in free space, based on experience at the HADES, the inductivity was assumed conservatively to be 50% higher. Aiming at moderate *Q*-values[13], resulting antenna properties summarized in Table 9 can be judged as reasonable: the amount of Cu to build the antenna is less than 550 kg, and the maximum achievable data rates from point of view of transmitter antenna design are between 19 and 33 sym/s.

Table 9: Properties of selected antenna diameters

transmitter antenna radius [m]	estimated antenna inductivity [mH]	wire resistance [Ohm]	antenna Cu mass [kg]	estimated max. data rate [sym/s]
500	12	2.8	543	19
250	6	1.4	271	20
125	4	1.1	87	33

In a third step, the required signal strength at the surface can be estimated. Based on an achieved sensitivity of 10 fT/√Hz, and aiming at ratio's between data rate and transmission frequency of about 1:15 (smallest ratio demonstrated 1:16, see Table 6), the required signal strength at the surface were computed (Eq. 5) and the results are summarized in Table 10. The data rates are in line with the estimated maximum data rate imposed by the transmitter antenna design (see Table 9), thus no limitation exists here with respect to the antenna radius.

Table 10: Estimated required signal strength at the surface for different data rates and bit error rates (BER)

data rate [sym/s]	transmission frequency [Hz]	estimated required signal strength at surface [fT]	
		BER = 0.1%	BER = 0.01%
5	75	212	299
10	150	299	422
15	250	366	517

In the last step, the power required to generate the required signal strength at the surface was computed. First, based on signal attenuation as a function of distance and loop diameter (Eq. 7 in [8]) and the attenuation by interactions with the geological medium as a function of the electrical conductivity (Eq. 11, Appendix A), the required transmitter antenna current was calculated. With the

[13] HADES demonstrations has taken place with *Q*-values of 5, but higher *Q*-values might be possible

calculated antenna current, the transmitter antenna's impedance (Table 9), and the selected data rates, the required transmitter power was computed and summarized for the highest data rates in Table 11.

Table 11: Estimated energy need for data transmission over 500 m of a highly conductive medium for a data rate of 15 sym/s and transmission frequency of 250 Hz

BER [%]	electrical conductivity [S/m]	required transmission energy [µWs/bit] 500 m loop	250 m loop	125 m loop
0.1	0.05	5.6	11	84
	0.033	2.2	4.4	34
	0.01	0.5	1.0	7.6
0.01	0.05	11	22	168
	0.033	4.5	8.7	67
	0.01	1.0	2.0	15

The above given example calculations show that when using a large antenna, high energy efficiencies can be achieved, with less than 0.1mWs per bit of transmitted data. Thus, when extrapolating the demonstrated results to selected disposal designs, it is obvious that the largest improvement of energy efficiency can be attributed to the area of the transmitter antenna. Because the magnetic moment is related to the surface area of the antenna (i.e. to the square of the radius), the application of a larger antenna (not demonstrated) presents greater potential for improving the antenna efficiency. In case of the experiments in the HADES, the antenna is about a factor of 100 smaller than the optimum size, leading to a major decrease of the performance of the transmission technique[14].

A second relevant factor that needs to be considered is the actual background noise in the projected frequency range on location: the energy need increases with the square of the required signal strength, e.g. by a factor of 25 in case of the HADES experiments. Other factors are less important (see Table 11).

4.2.2 Case II: generic Dutch disposal concept in rock salt

The generic Dutch disposal concept in rock salt is situated at a depth of 800 m, with the upper boundary of the rock salt dome situated at 300 m depth [18]. The conductivity values for the geosphere above the rock salt are assumed to be comparable to those depicted in Figure 4. Compared with the electrical conductivity of the surrounding geosphere, the conductivity of the host rock can be neglected. Overall, an average conductivity between 5 and 15 mS/m is assumed.

From Figure 37, transmission frequencies between 100 and 400 Hz can be derived, following the same reasoning as in the previous case.

[14] note that because field and strength power are also related to each other by a square law, a factor 100 decrease in loop antenna radius results in first estimation in a increase of the necessary power by a factor of 100'000'000 (the real advantage is smaller due to a number of complex factors)

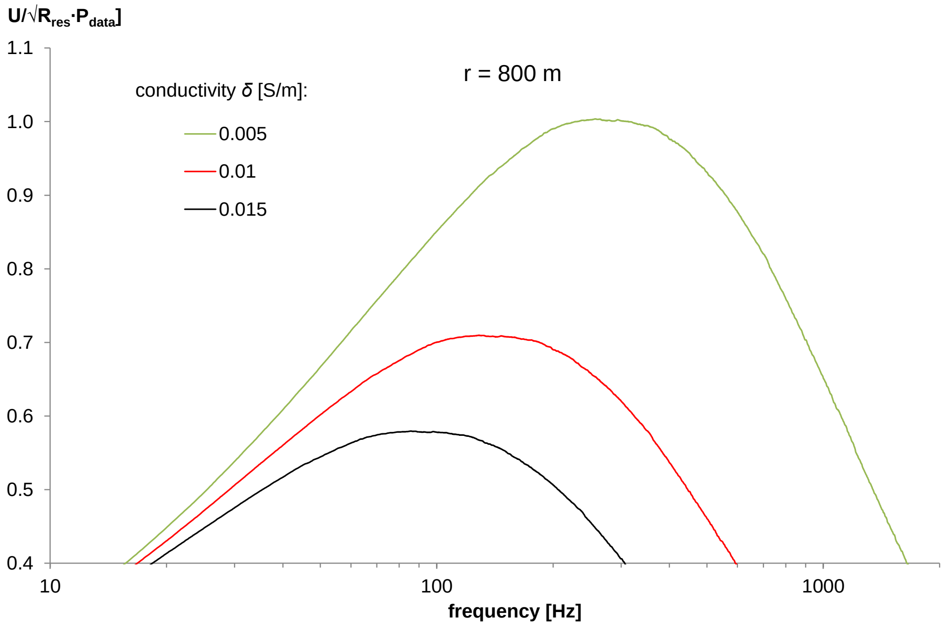

Figure 37: Transfer function for data transmission through a conducting medium for a resonant transmitter antenna, a transmission distance of 800 m and electrical conductivities between 0.005 and 0.015 S/m

In a second step, again transmitter antenna properties are defined. Three antenna radii were considered for this case, too: 800 m, 400 m and 200 m. For *Q*-values around 5, resulting antenna properties are summarized in Table 12.

Table 12: Properties of selected antenna diameters

transmitter antenna radius [m]	estimated antenna inductivity [mH]	wire resistance [Ohm]	antenna Cu mass [kg]	estimated max. data rate [sym/s]
800	19	9.7	402	39
400	9.4	4.8	201	41
200	4.4	2.2	113	39

The estimated required signal strength at the surface for data rate - transmission frequency ratios of about 1:15 are summarized in Table 13. Also here, the data rates are in line with the estimated maximum data rate imposed by the transmitter antenna design (see Table 12).

Table 13: Estimated required signal strength at the surface for different data rates and bit error rates (BER)

data rate [sym/s]	transmission frequency [Hz]	estimated required signal strength at surface [fT]	
		BER = 0.1%	BER = 0.01%
7	100	250	353
15	200	366	517
30	400	518	732

In the last step, the power required to generate the required signal strength at the surface was computed for the highest data rate (Table 14). The results show that also in this case data can be transmitted over a distance of 800 m with a reasonable amount of energy. A more detailed analysis of the results for the highest conductivity value of 0.015 mS/m (Table 15) show, that for lower transmission frequencies (and data rates) higher energy efficiencies can be obtained.

Table 14: Estimated energy need for data transmission over 800 m of a conductive medium for a data rate of 30 sym/s and transmission frequency of 400 Hz

BER [%]	electrical conductivity [S/m]	required transmission energy [µWs/bit]		
		800 m loop	400 m loop	200 m loop
0.1	0.015	85	165	743
	0.01	31	60	271
	0.005	9.4	0.46	2.1
0.01	0.015	170	329	1482
	0.01	62	120	540
	0.005	19	0.9	4.1

Table 15: Estimated energy need for data transmission over 800 m of a conductive medium with an (average) electrical conductivity of 0.015 mS/m and transmission frequencies between 100 and 400 Hz

BER [%]	transmission frequency [Hz]	required transmission energy [µWs/bit]		
		800 m loop	400 m loop	200 m loop
0.1	100	6.7	17	85
	200	13	34	165
	400	58	151	743
0.01	100	13	35	170
	200	26	67	329
	400	116	302	1482

In conclusion, for both disposal concepts, the estimated energy need is very promising. Considering that uncertainties of field propagation in the demonstration work are within a factor of 2 (thus a factor of 4 in terms of energy), energy efficiencies of <1mWs/bit must be achievable. Again, it must be noted that the major improvement of these cases compared to the demonstrated values are due to the (not demonstrated) larger transmitter antenna dimensions. Results of surface-surface experiments as discussed in Section 4.1 and their extrapolation in Table 8 give additional evidence that the estimated energy efficiencies of <1mWs/bit derived here are not too optimistic. However, in case of a disposal concept in rock salt, another major uncertainty arises from the fact that the horizontal extent of a salt dome is rather limited compared to the Boom Clay layer, while the propagation behaviour is based on the assumption of a horizontal stratified geosphere. This may potentially lead to a more complex propagation behaviour than in the case of a repository in Boom Clay, but an analysis of that situation is beyond the scope of the work performed.

5 Conclusions

In the previous chapters, the experimental work performed by NRG at the HADES URL is summarized, with the main objective of demonstrating the ability to transmit monitoring data wirelessly from a deep underground disposal facility to the surface. The transmission of data over larger distances (>100 m) of an electrically conductive medium is a challenging subject, because transmission by magneto-inductive techniques can only be realized at unfavourable low frequencies usually avoided for communication. The HADES was found to be a very suitable location in order to demonstrate the feasibility of the selected technique under conditions as expected for the Dutch generic disposal concept in Boom Clay: the high electrical conductivities of the transmission path between the HADES and the surface are comparable to the Dutch Case. However, the experimental conditions at Mol were not optimal with respect to three features:

- The size of the transmitter antenna was limited by the diameter of the HADES, leading to an antenna aperture far below optimum;
- Due to the presence of several on- and off-site power-lines, strong interferences exist on the surface above the HADES that impaired the reception of the transmitted data;
- Activities on-site (e.g. passing cars, shaft lift, construction works) lead to transient interferences that complicated statistical evaluation of data transmission experiments.

The experimental results demonstrated however, that by careful system design, data transmission through 225 m of a highly conducting geological medium is feasible. NRG has demonstrated at the HADES the wireless transmission of data through 225 m of an electrically highly conductive geological medium, at frequencies up to 1.7 kHz and with data rates up to 100 sym/s.

The energy efficiency of the transmission technique was identified in [8] as the major bottleneck for the application of this transmission technique in a post-closure situation. The amount of energy required to transmit data to the surface was within expectation, although due to the local conditions in Mol (limited space in the underground facility, strong interference aboveground) the capability to demonstrate the expected efficiency of the technique was limited. The overall efficiency of the developed technique was found to be quite promising: with 1Ws/bit demonstrated under the very challenging conditions present at the HADES, a few mWs/bit extrapolated from additional surface-surface experiments performed in a recreational area, and less than 1mWs/bit estimated for optimal conditions. It can be stated from the current point of view that it is in principle feasible to utilise this technology to transmit data in the post-closure phase. Estimation of the energy need in case of the Dutch generic disposal concept in Boom Clay, situated at 500 m depth, results in comparable numbers (<1 mWs of energy per bit of transmitted data). In other host rocks (rock salt, granite, Opalinus clay), even higher energy efficiencies can be achieved due to the lower electrical conductivities of these materials. However, there would be value in providing some additional experimental evidence for the efficiency of the technique when a large antenna is applied. This would require a different location than the HADES, preferentially at a relevant depth (>250 m) and with sufficient space to place a transmitter antenna of relevant dimension (loop radius >0.1 transmission distance).

A theoretical framework for the wireless transmission of data was developed within WP2.3 [8], and the experimental results were found to be consistent with the proposed framework. The analyses performed in [8] showed that, although some uncertainties exist and some parameters needed to be provided experimentally, the developed framework allows the estimation of general features and parameters required to set-up a transmission chain from a subsurface disposal facility to the surface. One of the major uncertainties identified was the propagation behaviour of the subsurface antenna in the extended near-field of a conducting half space. The experiments performed at the HADES showed that although the field vector differed from what was implied by the approximation equation used, the overall field strength was in close agreement to what was expected (within less than a factor of two).

In order to further substantiate the feasibility of this technology, additional research is necessary on the future on a number of topics:

- More clarity is needed on the amount of data that need to be transmitted in the post-closure phase and the duration of post-closure monitoring. The two cases defined in [8], Annex A, are a first estimation of the potential number of data. The transmission intervals and transmission periods to be expected in a future disposal situation should be examined more closely in order to be able to make a clear statement on the feasibility of post-closure monitoring.
- One of the main open questions discussed is the provision of electrical power in the post-closure case during extended periods of time (at least several decades). Several techniques were suggested, but at present neither a clear preference for a technique can be established nor has a detailed outline for a solution been provided. Essential to this discussion is also the overall period of post-closure monitoring.
- Additional work is needed in order to provide information on the long term durability/reliability of the components of the transmission technique. The current experimental set-up was used in order to provide the data necessary to support the findings of this report, but no effort was made to project or design a prototype or to make estimations on the reliability of the underground transmitter in the long term.
- The impact of the loss of a larger part of data at a certain transmission moment should be assessed. Because the frequency range used for transmission is rather 'vulnerable' to long-distance natural and man-made interferences (e.g. thunderstorms), it is necessary to evaluate if the loss of data is relevant or not and what potential countermeasures would be. Although several technical options exist, the aspects of simplicity and robustness of the transmission components and set-up should be weighed against data needs, in order to support durability and long-term reliability of the set-up.

Furthermore, envisaging the wireless transmission as only one element of an overall conceptual monitoring infrastructure, several other open topics can be identified:

- The integration of data-transmission techniques with other components of the monitoring infrastructure has not been discussed yet, nor the integration of data-transmission over different distances (e.g. through the borehole seals, between different section of the facility). Relevant questions include:
  - Whether data should be transmitted on demand, allowing for adapted measuring intervals dependent upon the previous outcomes, or considering it sufficient for the subsurface infrastructure to provide data at predefined intervals;

    - How the energy distribution of the overall monitoring infrastructure should be organized, how efficient and robust 'hibernation states' could be implemented, and how failing components could be detected and deactivated;
    - How wireless techniques applied on different scale could be coupled, and energy supply of the different units in the pre- and post-closure phase could be managed.
- The need to provide a bidirectional data-link between the disposal and the surface should be considered in the overall context of repository monitoring. Such a link can be technically realized in a comparable manner to what is presented in this report, but again simplicity and robustness of the set-up should be weighed carefully against possible advantages of a bidirectional link.
- The work described in this report may also serve as a basis for analysis if the wireless transmission of energy in order to supply monitoring equipment located behind barriers is generally feasible. Following the principles described, eventually making use of parts of the underground transmitter, an analysis should be conducted of the potential for such a technology to provide the data transmission unit and other parts of the monitoring equipment with energy.

Acknowledgements

We greatly acknowledge the kind support of Jan Verstricht and other members of the *EURIDICE* staff during our experimental work at the HADES URL in Mol, Belgium. NRG has received funding from the European Atomic Energy Community's Seventh Framework Programme (FP7/2007-2011) under grant agreement no 232598 and from the Ministry of Economic Affairs, Agriculture, and Innovation, The Netherlands.

Appendix A

This appendix presents a very condensed summary on the most important principles behind the transmission of data through the subsurface. The content is based on the NRG contribution to the *MoDeRn* Deliverable 2.3.1 [8], where derivations and a more in-depth analysis can be found.

The magnetic moment m_d of a loop antenna is a function of the loop area (A), the number of turns of the loop N and the current I:

$$m_d[A \cdot m^2] = A \cdot N \cdot I \quad \text{Eq. 6}$$

with the product *NI* also indicated as 'antenna aperture'.

The electric power *P* required to produce a current *I* at a given frequency *f* can be estimated by

$$P\,[W] = Z_l \cdot I^2 \quad \text{Eq. 7}$$

A low antenna impedance thus increases the efficiency of the transmitting antenna. The impedance of a loop antenna Z_l can be calculated by

$$Z_l[\Omega] = \sqrt{R_{res}^2 + (2\pi f \cdot L_l)^2} \quad \text{Eq. 8}$$

with the frequency independent ohmic resistance R_{res} is linearly related to the length of the wire and the cross section area, and the antenna's inductivity at the frequency *f* roughly approximated by

$$L_l[H] = \mu_0 \cdot \mu_r \cdot N^2 \cdot r_l (\ln \frac{8r_l}{r_w} - 1.75) \quad \text{Eq. 9}$$

with

μ_0	permeability constant (≈1.3·10-6 V·s/A·m)
μ_r	permeability [-] (≈ 1 for all materials considered here)
r_l	radius of the loop in [m]
r_w	radius of the wire in [m]

In case of a loop transmitting loop antenna in a deep geological disposal, with the receiver antenna located at the surface, the propagation between the buried transmitter antenna and a coaxial receiver antenna at the boundary at the distance *r* can be estimated by:

$$H_{radial} = \frac{m_d}{2\pi r^3} T_{radial} \quad \text{Eq. 10}$$

$$H_{vertical} = \frac{m_d}{2\pi r^3} T_{vertical} \quad \text{Eq. 11}$$

$$\left.\begin{matrix} T_{radial} \\ T_{vertical} \end{matrix}\right\} = \int_0^{\infty} \frac{x^3}{x + \sqrt{x^2 + iG^2}} \exp\left(-\sqrt{x^2 + iG^2}\right) \left\{\begin{matrix} J_1(xD) \\ J_0(xD) \end{matrix}\right. dx \qquad \text{Eq. 12}$$

where J_0 and J_1 are Bessel functions of the first kind, h the vertical and ρ the horizontal distance to the transmitter, σ the electrical conductivity, μ the magnetic permeability, $G=h\cdot(\sigma\mu 2\pi f)^{½}$, and $D=\rho/h$.

References

[1] Ministry of Heath, Spatial Planning and Environment (VROM). *Kabinetsstandpunt over de vraag of de diepe ondergrond mag en kan worden gebruikt voor het opbergen van afval*. Letter of the Minister van de Minister of Heath, Spatial Planning and Environment to the Lower House, Plenary Year 1992-1993, 's-Gravenhage, 14 May 1993

[2] Ministry of Economic Affairs, Agriculture and Innovation, Ministry of Foreign Affairs. *Joint convention on the safety of spent fuel management and on the safety of radioactive waste management. National Report of the Kingdom of the Netherlands*. Fourth review conference (May 2012). The Hague, September 2011

[3] MoDeRn, *Monitoring Developments for safe Repository operation and staged closure*, Annex I - “Description of Work”, Euratom Seventh Framework Programme Grant agreement no.: 232598, FP7-232598 – MoDeRn, July 1, 2009

[4] MoDeRn. *Technology Summary Report*. MoDeRn Deliverable, 2013, www.modern-fp7.eu

[5] IAEA. *Monitoring of Geological Repositories for High Level Radioactive Waste*. IAEA-TECDOC-1208, IAEA Vienna, 2001

[6] European Commission. *Thematic Network on the Role of Monitoring in a Phased Approach to Geological Disposal of Radioactive Waste. Final report*. Nuclear science and technology report EUR 21025 EN, 2004

[7] Verhoef, E., E. Neeft, J.B. Grupa, A.D. Poley, Outline of a disposal concept in clay, OPERA-PG-COV008, COVRA N.V., July 2011

[8] MoDeRn. *WP2. Development Report of Monitoring Technology*. MoDeRn Deliverable D2.3.1, 2013, www.modern-fp7.eu

[9] Lehner, G. *Elektromagnetische Feldtheorie für Ingenieure und Physiker*. 6th ed., Springer Verlag, Heidelberg, 2008

[10] Boisson, J.-Y. (ed.). *Catalogue of the characteristics of argillaceous rocks. OECD/NEA-RWMC/IGSC Working Group on Measurement & Physical Understanding of Groundwater Flow Through Argillaceous Media (Clay Club)*, Paris, France, 2003

[11] Verstricht, J. *Magneto-Inductive tests at the Mol site. Additional site data*. EIG EURIDICE, August 31, 2005

[12] Shope, S.M. *Electromagnetic Surface Fields Due to a Magnetic Dipole Buried in a Three-Layered Earth*. Bureau of Mines report of investigations 8702, United States Department of Interior, 1982

[13] Harris, F. J. 1978. *On the Use of Windows for Harmonic Analysis with the Discrete Fourier Transform*. Proceedings of the IEEE, 66 (1), p.172-204

[14] Spies, B.R. and F.C. Frischknecht. 1992. *Electromagnetic sounding*. In: Nabighian, I. and N. Misac (ed.). Electromagnetic methods in applied geophysics, Society of Exploration Geophysists, p.248-425

[15] Rahnema, M. 1993. *Overview Of The GSM System and Protocol Architecture*. IEEE Communications Magazine, p.92-100

[16] Wikipedia. *Terrestrial Trunked Radio*. *http://en.wikipedia.org/wiki/TETRA*

[17] Martinez, P. *PSK31: A New Radio-Teletype Mode*. Radio Communication, January 1999
[18] Heijdra, J.J. and J. Prij. Concept ontwerp terughaalbare berging in steenzout. Eindrapport 1996 METRO I. ECN report ECN-C--96-087, Netherands Energy Research Foundation (ECN), Petten, 1997